Modeling phylogenetic biome shifts on a planet with a past

Michael J. Landis[1,2,*], Erika J. Edwards[2,3], and Michael J. Donoghue[2,3]

[1] *Department of Biology, Washington University in St. Louis, One Brookings Drive, St. Louis, Missouri 63130, USA*

[2] *Department of Ecology & Evolutionary Biology, Yale University, PO Box 208106, New Haven, Connecticut 06520, USA*

[3] *Division of Botany, Yale Peabody Museum of Natural History, P.O. Box 208118, New Haven, Connecticut 06520, USA*

[*] *Email correspondence: michael.landis@wustl.edu*

Abstract.—The spatial distribution of biomes has changed considerably over deep time, so the geographical opportunity for an evolutionary lineage to shift into a new biome may depend on how the availability and connectivity of biomes has varied temporally. To better understand how lineages shift between biomes in space and time, we developed a phylogenetic biome shift model in which each lineage shifts between biomes and disperses between regions at rates that depend on the lineage's biome affinity and location relative to the spatiotemporal distribution of biomes at any given time. To study the behavior of the biome shift model in an empirical setting, we developed a literature-based representation of paleobiome structure for three mesic forest biomes, six regions, and eight time strata, ranging from the Late Cretaceous (100 Ma) through the present. We then fitted the model to a time-calibrated phylogeny of 119 *Viburnum* species to compare how the results responded to various realistic or unrealistic assumptions about paleobiome structure. Ancestral biome estimates that account for paleobiome dynamics reconstructed a warm temperate (or tropical) origin of *Viburnum*, which is consistent with previous fossil-based estimates of ancestral biomes. Imposing unrealistic paleobiome distributions led to ancestral biome estimates that eliminated support for tropical origins, and instead inflated support for cold temperate ancestry throughout the warmer Paleocene and Eocene. The biome shift model we describe is applicable to the study of evolutionary systems beyond *Viburnum*, and the core mechanisms of our model are extensible to the design of richer phylogenetic models of historical biogeography and/or lineage diversification. We conclude that biome shift models that account for dynamic geographical opportunities are important for inferring ancestral biomes that are compatible with our understanding of Earth history.

(Keywords: phylogenetics, ancestral states, biome shifts, niche conservatism, historical biogeography)

INTRODUCTION

Biomes are ecologically and climatically distinct species assemblages that vary in size, shape, and continuity across geographical regions, in large part due to regional differences in temperature, precipitation, seasonality, altitude, soil types, and continentality (Whittaker 1970; Wolfe 1985; Olson et al. 2001; Mucina 2019). The diversity of biomes occupied by particular lineages also varies considerably, with some clades exhibiting strict associations with particular biomes, and others showing multiple transitions between biomes over time (Donoghue and Edwards 2014). Although it is accepted that clade-wide variation in regional biome occupancy was generated and is maintained by evolutionary forces including speciation, extinction, dispersal, and adaptation to new biomes, it remains difficult to estimate exactly when, where, and under what conditions phylogenetic lineages first shifted into the biomes that their descendants inhabit today.

In current practice, ancestral regions and biome affinities are often estimated independently of one another, and then relationships between regions and biomes are compared post hoc (e.g., Crisp et al. 2009; Weeks et al. 2014). Although such studies yield important evolutionary insights, the estimates themselves do not account for how lineages might move between regions or adapt to newly encountered biomes given the temporally variable spatial configuration of biomes across regions. Conceptually, how a biome is geographically distributed should influence how easily a lineage might disperse into a new region or shift into a new biome, an effect Donoghue and Edwards (2014) termed geographical opportunity. One strategy to model the effect of geographical opportunity first defines discrete regions that are exactly coincident with modern day biomes, and then

assumes that species within a given region occur within the corresponding biome. Cardillo et al. (2017) carried out such an analysis in studying the biogeography of the Australian plant clade, *Hakea* (Protaceae), using method features developed by Matzke (2014), where total regional area and shared perimeter lengths tuned dispersal rates between bioregions. This innovative strategy depends crucially on the uniformity of biome composition within each region. Larger, discrete regions may very well be dominated by a single biome type, yet still be composed of assorted dominant, subdominant, and marginal biome types at local scales.

More importantly for our purposes, defining geographical opportunity based on modern biome features (such as area and shared perimeter), may be problematic in instances where the spatial distribution of biomes has changed considerably over time, since those changes should also influence when and where ancestral lineages shift between regions and/or biomes. For example, if woodlands dominated a particular region until the rise of grasslands, that might inform when a grassland-adapted lineage first dispersed into that region. That is, if the presences or absences of biomes among regions influence modern species ranges, then temporal variation in regional biome availability should similarly influence our models of range evolution.

To model how paleoecological dynamics might influence range evolution, Meseguer et al. (2015) fitted ecological niche models (ENMs) to fossil data so as to limit the connectivity between regions for biogeographical models that estimate ancestral ranges (Ree and Smith 2008). While this strategy is quite promising, its current form requires that the clade under study (*Hypericum* of Hypericaceae, in their case) has a sufficiently rich fossil record over space and time to inform the ENM. It also assumes that all lineages face

84 the same, broad ecological limitations to range evolution, independent of what particular
85 biome affinity each lineage possesses at a given moment. Although the quality of the fossil
86 record is largely out of our control, the second assumption could be relaxed: ideally, if a
87 clade contains sub-lineages that specialize in both woodland and in grassland habitats, any
88 particular lineage's range should be principally limited by the availability of the specific
89 biome to which that lineage is adapted, rather than being constrained based on a broader,
90 clade-wide average of grassland and woodland lineages.

91 In this paper, we aim to address the aforementioned challenges facing current
92 phylogenetic models of biome shifting by incorporating four key properties: (1) that biome
93 shifts and dispersal events share a common state space over biomes and regions, (2) that
94 any discrete region may contain a number of different biomes, (3) that the geographical
95 structure of biomes within and between regions can vary over time, and (4) that lineages
96 adapted to different biomes and located in different regions will experience different
97 dispersal rates between regions and different shift rates into new biomes. We begin by
98 introducing a graph-based approach to characterize the availability, prevalence, and
99 connectivity of regional biomes through time, building on the framework introduced by
100 Landis (2017). We then develop an event-based evolutionary process using a time-
101 stratified continuous-time Markov chain that models biome shifts and dispersal given the
102 ways in which biome distributions have changed over time. Because the exact influence of
103 extrinsic geographical factors and/or ecological structure is bound to vary from clade to
104 clade, the degree of influence of such features on the evolutionary model are treated as free
105 parameters to be estimated from the data itself.

106 To explore the possible importance of paleobiome structure on lineage movements
107 among biomes, we apply our model to *Viburnum*, a clade of ~165 species that originated in
108 the Late Cretaceous and are today found in tropical, warm temperate, and cold temperate
109 forests throughout Eurasia and the New World. We generated paleobiome graphs for these
110 three mesic forest biomes across six continental regions for eight major time intervals over
111 the past hundred million years. Fitting the model to our *Viburnum* dataset all-but-
112 eliminates the possibility of a cold temperate origin of the clade. This is consistent with our
113 understanding of the important biogeographic role of a "boreotropical" flora (see below)
114 during the Paleocene and Eocene, and with our recent fossil-based ancestral biome
115 estimates in *Viburnum* (Landis et al. 2019).

116 ## METHODS

117 ### *Viburnum phylogeny and biogeography*

118 *Viburnum* (Adoxaceae) is a clade of ~165 extant plant species that originated just
119 before the Cretaceous-Paleogene (K-Pg) boundary, roughly 70 Ma. Previous studies of
120 phylogenetic relationships (Clement et al. 2014; Spriggs et al. 2015; Eaton et al. 2017) and
121 divergence times (Spriggs et al. 2015; Landis et al. 2019) provide a firm basis for
122 understanding the order and timing of lineage diversification events in *Viburnum*. In this
123 study, we focus on a subsample of 119 *Viburnum* species with relationships that are highly
124 supported by phylogenomic data (Eaton et al. 2017; Landis et al. 2019) and whose
125 divergence times were time-calibrated under the fossilized-birth death process (Heath et
126 al. 2014) as described in Landis et al. (2019).

127 *Viburnum* species occupy six continental-scale regions: Southeast Asia, including the
128 Indoaustralian Archipelago and the Indian subcontinent; East Asia, including China,

129 Taiwan, and Japan; Europe, including the North African coast, portions of the Middle East,
130 and the Azores and the Canary Islands; a North American region north of Mexico; a Central
131 American region that includes Mexico, Cuba, and Jamaica; and the South American Andes.
132 The choice of these biogeographic regions is discussed in more detail in Landis et al.
133 (2019). Briefly, these regions were selected because: (1) each is an area of *Viburnum*
134 species/clade endemism; (2) there are no individual *Viburnum* species that occur in more
135 than one of these regions; and (3) there are significant barriers to the migration of
136 viburnums between these regions today and in the relevant past. As a concrete example,
137 consider our recognition of North America and of Mexico, Central America, and the
138 Caribbean as two distinct biogeographic regions for *Viburnum*. Multiple *Viburnum* species
139 are endemic to the forests in each of these regions, and none of these species spans
140 between them. Importantly, for mesic forest plants such as *Viburnum*, these two regions
141 are entirely separated from one another by an extensive zone of low-lying arid lands in
142 southeastern Texas and northeastern Mexico, with vegetation generally classified as xeric
143 shrubland or mesquite-chaparral savanna. These areas are uninhabitable by viburnums
144 today, and probably have not been accessible to these plants since widespread drying and
145 the spread of C4 grasses commenced by at least the late Miocene (e.g., Godfrey et al. 2018).
146 Using our criteria, the most difficult division is between the southeast Asian and eastern
147 Asian regions. Although these do both harbor endemic species/clades, and these species
148 are adapted to different environmental conditions, there are now, and have been in the
149 past, opportunities for north-south migration between mesic forests of the two regions.
150 Finally, we note that our biogeographic regions are not strictly defined in terms of tectonic
151 plates as they do not determine the movements and distributions of *Viburnum*. Thus, based

152 on the criteria above, we split the vast Eurasian plate into a European region and two Asian
153 regions. Likewise, the boundary between the North American and the Caribbean plates
154 appears to have had no impact on *Viburnum* movements as there are individual species
155 (e.g., *V. hartwegii*) that span the two.

156 Across those regions, living viburnums are affiliated with mesic forest biomes and
157 show widespread parallel evolution of leaf form, leafing habit, and physiology coincident
158 with transitions between warmer and colder biomes (Schmerler et al. 2012; Chatelet et al.
159 2013; Spriggs et al. 2015; Scoffoni et al. 2016; Edwards et al. 2017). Five extinct *Viburnum*
160 lineages are known by their fossil pollen grains recovered from North American and
161 European locales. Four of these fossils are older samples (48 to 33 Ma) from paleofloral
162 communities that we previously judged to be warm temperate or subtropical (Landis et al.
163 2019). For our analyses in this study, we defined three mesic forest biomes based on
164 annual temperatures and rainfall patterns (Edwards et al. 2017). Tropical forests have high
165 temperatures and precipitation year-round, showing little seasonality. Warm temperate
166 forests, which include paratropical, lucidophyllous, and cloud forests, vary seasonally in
167 temperature and precipitation, but do not experience prolonged freezing temperatures
168 during the coldest months. Cold temperate forests also experience seasonal temperatures
169 and precipitation, but average minimum temperatures drop below freezing in at least one
170 of the coldest months.

171 Because we are interested in how biome states and regional states evolve in tandem,
172 we constructed a set of $3 \times 6 = 18$ compound states that we call biome-region states.
173 Throughout the paper, we identify the biome-region state for a lineage in biome state i and
174 region state k with the notation (i,k). However, in practice, we encode biome-region states

as integers with values from 1 to 18. Biome-region state codings for *Viburnum* are translated from Landis et al. (2019), though here we combine cloud forests and warm temperate forests into a single warm temperate category.

All of the 119 Viburnum species we included in our analysis are found in a single biome, except for two East Asian (*V._chinshanense* and *V._congestum*) and one North American (*V. rufidulum*) species, which reside in forests possessing both warm and cold temperate elements. Those three species were coded as ambiguous for the relevant biome-region states. While it may be more accurate to describe those species as occupying multiple biomes, the model that we will soon define assumes that lineages occupy only one biome-region state at any given time. The biome-region character matrix and the time-calibrated phylogeny for *Viburnum* that we used are hosted on DataDryad (LINK).

Model overview

Our aim is to model a regional biome shift process that allows changes in the spatiotemporal distribution of biomes to influence the likelihood of a lineage shifting between biomes and dispersing between regions. This process can be described in terms of interactions between two fundamental subprocesses: the biome shift process and the dispersal process.

The biome shift process models when and where lineages shift into new biome types. The probability of a biome shift clearly depends on intrinsic and extrinsic factors that govern how readily a lineage might adapt to the conditions in a new biome, which involves a myriad of factors that we do not fully explore here. Rather, we focus specifically on modeling the effect of geographical opportunity on biome shifts (Donoghue and

198 Edwards 2014). For example, it is plausible that a species inhabiting the warm temperate
199 forests of Europe might have shifted into the tropical biome during the Early Eocene, a
200 period when tropical rain forests could be found at latitudes as extreme as 60° N. In
201 contrast, a biome shift within Europe from a warm temperate to a tropical biome would be
202 less likely today or during any time after the global cooling trend that began with the
203 Oligocene.

204 The dispersal process models how lineages move between regions. The rate of
205 dispersal between regions should depend on how connected those regions are for a given
206 biome affinity. Returning to the Europe example, a tropical lineage in Southeast Asia might,
207 all else being equal, have a relatively high dispersal rate into Europe during the Early
208 Eocene, when Europe was predominantly tropical and warm temperate, as compared to
209 today, when Europe is dominated by temperate and boreal forests. This rate would,
210 however, also be influenced by geographical connectivities at the time. In this case, the
211 existence of the Paratethys Sea and the Turgai Strait may have influenced plant migrations
212 at different latitudes during the Eocene, although the fragmented northern shore of the
213 Tethys Sea facilitated the movement of tropical and subtropical plants throughout much of
214 that period (Tiffney 1985a, b; Tiffney and Manchester 2001).

215 How the biome shift and dispersal processes may behave in response to an evolving
216 biome structure is depicted in Figure 1. By characterizing known features of paleobiome
217 structure (Fig. 1A) into adjacency matrices (Fig. 1B), we can differentiate between probable
218 and improbable phylogenetic histories of biome shifts and dispersal events (Fig. 1C) based
219 on time-dependent and paleobiome-informed biome shift rates (Fig. 1D) and dispersal
220 rates (Fig. 1E). Of the two regional biome shift histories in Figure 1C, the first history

221 invokes three events that are fully congruent with the underlying paleobiome structure.
222 The second history requires only two events, yet those events are incongruent with the
223 paleobiome structure. But which regional biome shift history is more probable? Assigning
224 probabilities to histories must depend not only on the phylogenetic placement and age of
225 the regional biome shift events, but also on the degree to which the clade evolves in a
226 paleobiome-dependent manner. We later return to how this unknown behavior of the
227 evolutionary process may be estimated from phylogenetic data, only after we define a
228 probabilistic model for the process.
229
230 *An evolving spatial distribution of biomes through time*
231 Biome availability and connectivity has evolved over time. We summarize these
232 dynamics with a series of time-dependent graphs that are informed by the paleobiological
233 and paleogeographical literature (Fig. 2). To define our paleobiome graphs, we consulted
234 global biome reconstructions generated by Wolfe (1985), Morley (2000), Graham (2011,
235 2018), Fine and Ree (2006), Jetz and Fine (2012), and Willis and McElwain (2014) which
236 we then corroborated with biome reconstructions quantitatively estimated using the
237 BIOME4 model (Prentice et al. 1992; Kaplan et al. 2003).
238 The BIOME4 reconstructions we obtained are 1-degree global rasters that classify
239 each cell (location) as one of 27 possible biomes. BIOME4 biomes are inferred from
240 assorted botanical and climatological information (observed or imputed) that represents a
241 given time interval. For each BIOME4 reconstruction, we interpreted the 11 forest biomes
242 as approximations of the availability and connectivity of mesic forest biomes among
243 regions, then compared those features to our literature-based reconstructions. Previously

244 published BIOME4 reconstructions were available for times corresponding to the Early-
245 Mid Eocene (Herold et al. 2014), the Late Ecoene and the Oligocene (Pound and Salzmann
246 2017), the Mid-Late Miocene (Pound et al. 2011, 2012), and the Pliocene (Salzmann et al.
247 2008; Salzmann, Haywood, and Lunt 2009). For time intervals that lacked published
248 BIOME4 reconstructions, we compared our paleobiome maps to unpublished
249 reconstructions provided by P. J. Valdes (pers. Comm.) that were built from proprietary
250 data. Our impression was that BIOME4 reconstructions tended to infer more arid and fewer
251 forest biomes than was generally supported by the paleobotanical literature. For example,
252 the BIOME4 reconstruction inferred that the Amazon contained more xeric shrubland than
253 tropical forest at the present. As such, we took presences of mesic forests under BIOME4 as
254 conservative estimates of their true distributions. That being said, the majority of
255 literature-based and BIOME4 reconstructions shared two important features: (1) the high
256 degree of availability and connectivity among tropical and warm temperate biomes in the
257 Northern Hemisphere before the Oligocene, and (2) the sudden rise of cold temperate
258 forests concomitant with the disappearance of many tropical forests, beginning with the
259 Oligocene.

260 We classified the availability and connectivity of biomes within regions into three
261 categories of features—strong, weak, and marginal—that were appropriate to the scale of
262 the regions and the precision of the ancestral biome estimates. Biomes with a strong
263 presence displayed ≥25% regional coverage, biomes with a weak presence covered <25%
264 of a region, while biomes with marginal presence covered <1% of a region. Likewise, the
265 connectivity of a biome between two regions at a given time is scored as either strong,
266 weak, or marginal, depending on how continuously biomes are inferred to have been

267 distributed near regional adjacencies. For example, the modern distribution of the cold
268 temperate biome throughout East Asia and Europe is consistent with strong connectivity,
269 while North America is only weakly connected to cold temperate Eurasian biomes through
270 its fragmented and transient arctic connections. Independent of the distribution of biomes,
271 we similarly scored the geographical connectivity between regions as strong, weak, and
272 marginal, using the equivalent of the modern connection between Central and South
273 America through the Isthmus as Panama to minimally qualify as strong connectivity, and
274 distances between modern Europe and North America to represent weak connectivity. The
275 geographical connectivity between two regions is, generally, at least as strong as the
276 strongest biome-dependent connection for those same regions. Together, the availability
277 and connectivity for each region, each biome, and each time interval is encoded into a
278 series of paleobiome graphs, which we later use to define the rates at which biome shift
279 and dispersal events occur.

280 Our paleobiome graphs capture several important aspects of how mesic forest
281 biomes moved and evolved (Fig. 2). The Late Cretaceous through the Paleocene and Early
282 Eocene was a prolonged period of warm, wet conditions during which the poles had little to
283 no ice. Throughout that time, tropical forests were prevalent in all six of our regions, while
284 warm temperate forests were widespread only throughout East Asia, Europe, and North
285 America. The Eocene witnessed the emergence of a so-called boreotropical flora, which
286 contained a curious mixture (from our modern vantage point) of tropical and temperate
287 plant genera (Wolfe 1975; Tiffney 1985a, b). This largely broadleaved evergreen forest
288 type appears to have spread widely around the northern hemisphere via the Beringia Land
289 Bridge, the North Atlantic Land Bridge, and the Tethys Sea (Tiffney 1985 a, b; Wolfe 1985;

290 Morley 2000; Willis and McElwain 2014; Graham 2011, 2018; Baskin and Baskin 2016),
291 and to have persisted through the Mid/Late Eocene. With the Oligocene, the opening of the
292 Drake Passage and the closure of the Tethys Sea redirected global ocean currents. Together
293 with steep declines in atmospheric CO_2 levels, this ushered in cooler and drier conditions
294 worldwide. The ensuing global climatic changes progressively restricted tropical forests to
295 more equatorial regions, inducing the disjunction we find among modern tropical forests
296 (Latham and Ricklefs 1993; Wiens and Donoghue 2004; Donoghue 2008). As the
297 boreotropical forests receded, they were first replaced by warm temperate forests, and
298 then eventually by cold temperate and boreal forests. Following this global revolution of
299 biome structure, connectivity between Old World and New World tropical forests never
300 again matched that of the Paleocene-Eocene boreotropical beltway.

301 We illustrate how a lineage might evolve with respect to different distributions of
302 biomes within and between regions over time with the aid of Figure 2. A lineage that freely
303 disperses between regions and shifts between biomes, regardless of the historical
304 condition of the planet, might transition between regions under fully connected matrices
305 (Uninformative, first column). Lineages that are only dispersal-limited by terrestrial
306 connectivity disperse under the adjacency constraints encoded in the second column of
307 matrices (Geographical, second column). However, lineages that are dispersal-limited by
308 biome availability and connectivity might disperse according to the paleobiome patterns
309 shown in the third, fourth and fifth columns (tropical, T; warm temperate, W; and cold
310 temperate, C). For example, a lineage that is strictly adapted to the warm temperate biome
311 would disperse according to the warm temperate series of paleobiome graphs (fourth
312 column). If that lineage shifted its affinity from a warm temperate to a tropical biome, that

313 lineage would thereafter shift between biomes and disperse between regions under the
314 adjacency matrix structures of the tropical biome (third column) until the lineage next
315 shifted biomes. However, biome shift rates also should depend on what biomes are locally
316 accessible. For example, a North American lineage would have the geographical
317 opportunity to shift from warm temperate into tropical biomes during the Paleocene, an
318 epoch when both biomes have strong presences in North America. But North American
319 tropical forests decline and then disappear throughout the Oligocene and Miocene,
320 extinguishing the opportunity for such a biome shift during more recent times. The next
321 section formalizes how we model the complex interactions between biomes, regions,
322 phylogeny, and time with these dynamics in mind.
323
324 *A time-stratified regional biome shift model*
325 The regional biome shift process may be viewed as a model that defines the
326 interactions (if any) of its two subprocesses, the biome shift process and the dispersal
327 process. We model biome shifts using a simple continuous-time Markov chain (CTMC) with
328 time-stratified rates (i.e. piecewise constant time-heterogeneous rate matrices; Ree et al.
329 2005; Buerki et al. 2011; Bielejec et al. 2014; Landis 2017). Because transition rates
330 between regions depend in part on a lineage's biome affinity, and rates of shifting between
331 biomes depend in part on a lineage's geographical location, the two characters do not
332 evolve independently. To impose interdependence between biomes and regions, we define
333 a rate matrix over the compound state space by modifying the approach of Pagel (1994),
334 while also drawing on insights pioneered in newer trait-dependent models of discrete

335 biogeography (Sukumaran et al. 2015; Sukumaran and Knowles 2018; Matos-Maraví et al.
336 2018; Lu et al. 2019; Klaus and Matzke 2019).

337 Accordingly, we define the CTMC to operate on the compound biome-region state,
338 (i, k), where i is the biome and k is the region. With this in mind, our goal is to compute the
339 probability of a lineage transitioning from biome i in region k to biome j in region l, or
340 (i, k) into (j, l). First, we take $\beta_{i,j}$ to model the shift rate between biomes i and j, and $\delta_{k,l}$ to
341 model the dispersal rate between regions, $\delta_{k,l}$. Importantly, the values of β and δ
342 themselves do not directly depend on time. We eventually multiply these base rates by
343 time-dependent paleogeographical and paleoecological factors represented in our time-
344 stratified (or epoch) model.

345 Computing the transition probabilities for an time-stratified model requires that we
346 define an instantaneous rate matrix $Q(m)$ for any supported time interval, m. Following
347 Landis (2017), we define the rate matrix $Q(m)$ as the weighted average of several rate
348 matrices, each capturing different paleogeographical features

349 $$Q(m) = w_U Q_U + w_G Q_G(m) + w_B Q_B(m).$$

350 The three matrices on the right-hand side of Equation 1 are the (paleogeographically)
351 uninformative rate matrix, Q_U, the geographical rate matrix, Q_G, and the biome rate matrix,
352 Q_B. In reference to Figure 2, we wish to learn the relative influence of the uninformative
353 (first column), geography (second), and biome (third, fourth, or fifth) matrix features on
354 the biome shift process. Supplement 1 demonstrates how rate matrix values are computed
355 for a toy example with two regions and two biomes.

356 The first rate matrix (Q_U) may be considered as an uninformative rate matrix that
357 sets the relative transition rates between all pairs of regions, and separately between all
358 pairs of biomes, as time-independent and context-independent,

359 $$[Q_U]_{(i,k),(j,l)} = \begin{cases} \beta_{i,j} & \text{if biome shift } (i \neq j) \\ \delta_{k,l} & \text{if region shift } (k \neq l) \\ 0 & \text{if biome and region shift } (i \neq j \text{ and } k \neq l) \end{cases}$$

360 The effect is that biome shifts between biomes i and j follow the rates $\beta_{i,j}$ and dispersal
361 events follow the rates $\delta_{k,l}$ regardless of the age of a lineage or the lineage's biome-region
362 state. As we develop rate matrices for geography (Q_G) and biomes (Q_B) below, the second
363 role for Q_U is that it allows for lineages to disperse or shift regardless of whether the
364 connectivity/availability of the involved regions or biomes are scored as strong, weak, or
365 marginal.

366 Because we do not know precisely what, if any, influence strong, weak, and marginal
367 features should exert upon the dispersal or biome shift processes, we estimate the relative
368 effects of those features across all adjacency matrices, the geographical adjacency matrix,
369 A_G, and the biome adjacency matrices, A_T, A_W, and A_C, for the tropical, warm temperate,
370 and cold temperate biomes, respectively (Fig. 2). Specifically, we assign the fixed values of
371 0 and 1 to marginal and strong features, respectively, then assign all weak features one
372 shared intermediate value, estimated as $0 < \mathrm{y} < 1$. In effect, y controls the degree of
373 contrast of medium-colored cells across all adjacency matrices in Figure 2. For example,
374 tropical connectivity during the Late Cretaceous is represented by the adjacency matrix
375 $A_T(1)$. At that time, tropical connectivity between East and Southeast Asia is strong
376 ($[A_T(1)]_{\mathrm{EAs,SEAs}} = 1$), connectivity between East Asia and Europe is weak
377 ($[A_T(1)]_{\mathrm{EAs,Eur}} = \mathrm{y}$), and connectivity between East Asia and South America is marginal

$([A_T(1)]_{\mathrm{EAs,SAm}} = 0)$. Future studies may find that one can model and reliably estimate separate values of y for different features, even though we do not investigate this possibility at present.

The second rate matrix (indexed G for geography, Q_G) is structured according to biome-independent paleogeographical features, such as the simple terrestrial connectivity between regions. Connectivity is encoded as either as strong, weak or marginal in the adjacency matrix, $A_G(m)$.

$$[Q_G(m)]_{(i,k),(j,l)} = \begin{cases} \beta_{i,j} & \text{if biome shift } (i \neq j) \\ \delta_{k,l} \times [A_G(m)]_{k,l} & \text{if region shift } (k \neq l) \\ 0 & \text{if biome and region shift } (i \neq j \text{ and } k \neq l) \end{cases}$$

The third rate matrix (indexed B for biome, Q_B) defines the shift rates between biomes and the dispersal rates between regions to depend on the spatiotemporal distribution of biomes. A lineage's biome shift rate depends on whether the receiving biome, j, has a strong, weak, or marginal presence in the region it currently occupies, k. Likewise, the dispersal rate for a lineage that is currently adapted to biome type i depends on whether the source region, k, and destination region, l, share a strong, weak, or marginal connection.

$$[Q_B(m)]_{(i,k),(j,l)} = \begin{cases} \beta_{i,j} \times \left[A_j(m)\right]_{k,k} & \text{if biome shift } (i \neq j) \\ \delta_{k,l} \times \left[A_j(m)\right]_{k,l} & \text{if region shift } (k \neq l) \\ 0 & \text{if biome and region shift } (i \neq j \text{ and } k \neq l) \end{cases}$$

It is crucial to recognize that $Q_B(m)$ defines shift rates involving biome j to depend on the adjacency matrix for biome j during time interval m. This key property means that lineages currently adapted to biome j disperse with rates according to the interregional

397 connectivity of biome j, and lineages newly adapting to biome j do so at a rate depending
398 on the local availability of biome j.

399 The transition rates (and probabilities) between biome-region pairs are not
400 expected to be symmetric or equal across time intervals. For example, if biome j first
401 appears in region k during time interval $m+1$, then we would potentially see an increase
402 in the biome shift rate into biome j, i.e. $[Q(m)]_{(i,k),(j,k)} < [Q(m+1)]_{(i,k),(j,k)}$. Nor are
403 transition rates necessarily symmetric or equal within a given time interval. If region k
404 contains biome i during time interval m, but region l does not, then we might find that
405 lineages adapted to biome i disperse less easily from k into l than l into k, i.e.
406 $[Q(m)]_{(i,k),(i,l)} < [Q(m)]_{(i,l),(i,k)}$. Similarly, if region k contains biome i but not biome j
407 during time interval m, then lineages inhabiting region k will tend to shift less easily from
408 biome i into j than from j into i, i.e. $[Q(m)]_{(i,k),(j,k)} < [Q(m)]_{(j,k),(i,k)}$.

409 Fluctuating asymmetries in the rates over time means that each biome-region state
410 may exhibit different source-sink dynamics across that timescale. During a period of low
411 accessibility, a biome-region state might rebuff immigrants and lose occupants when acting
412 as a source, but then gain and retain inhabitants during a later phase should that biome-
413 region become a local refugium when acting as a sink (Goldberg et al. 2005). These
414 fluctuating source-sink dynamics may be characterized by the stationary distribution,
415 which defines the expected proportion of lineages found in each biome-region state
416 assuming lineages evolve along an infinitely long branch within a given time interval.
417 Biome-regions that are easy to enter and difficult to leave tend towards higher stationary
418 probabilities for a given time interval.

419 We approximate the stationary probability for biome i in region k during time
420 interval m with

421 $$\pi(m)_{(i,k)} = \left[e^{\mu Q(m)}\right]_{1,(i,k)}$$

422 where μ is a rate taken to be sufficiently large that stationarity is reached. Note that the
423 bracketed term on the righthand side of the equation is the transition probability matrix
424 for changes between biome-region pairs. In theory, when μ is large, all rows in this matrix
425 have arbitrarily similar transition probabilities, which lets us take any row (i.e. the first
426 row) to represent the stationary probabilities.

427 The time-dependent source-sink dynamics in Figure 3 show how the availability of
428 and connectivity between regional biomes structures each time interval's stationary
429 distribution. Stationary probabilities before the Oligocene tend to favor tropical biomes in
430 all regions, but favor cold temperate biomes afterwards. This means that if the historical
431 spatial structure of biomes is relevant to biogeography, then lineages originating in the
432 Paleogene would more likely be adapted to tropical than to cold temperate forests simply
433 because cold temperate forests were a more marginal biome during that period of Earth's
434 history.

435 We can now completely define the time stratified rate matrix, $Q(m)$, and the
436 stationary frequencies at the root of a phylogeny, $\pi(m_{root})$, where m_{root} is the time
437 interval corresponding to the root node age. Together, these model components let us
438 compute the probabilities of lineages transitioning from one biome-region pair to another
439 while accounting for the spatiotemporal dynamics of biomes, and thus compute the
440 phylogenetic model likelihood with the discrete state pruning algorithm (Felsenstein
441 1981).

Now that we have fully defined the model, there are several implicit properties that are worth stating explicitly. First, a lineage cannot both shift its biome affinity and disperse into a new region in the same moment of time; one event is needed for each transition, and so event order matters. While we think this assumption is reasonable in many cases, including in *Viburnum*, it is certainly conceivable that region and biome shifts could occur simultaneously. We elaborate on this point in the Discussion, but note here that it would be possible to explore the effect of modeling such paired transitions by adapting parameterizations designed for multiple-nucleotide substitution codon models (Koisol et al. 2007). Second, the relative importance of the matrix feature weights (w_U, w_G, w_B) and of the weak availability/connectivity weight (y) are estimated from the data: the matrix $Q(m)$ reduces to the uninformative matrix, Q_U, when $w_U = 1$, while the importance of the historical structure of biomes is most pronounced when w_B is large compared to other w and y parameters. Third, the process models lineages as being predominantly present in a single region and biome at a time without influencing speciation or global extinction rates, which are assumptions we made both to simplify the exposition of the method, but also to reduce computational burden. The Discussion brings more attention to all of these properties.

Bayesian inference

The Bayesian posterior density was estimated using the Markov chain Monte Carlo (MCMC) algorithm implemented in RevBayes (Höhna et al. 2016). RevBayes scripts and datasets are available at http://github.com/mlandis/biome_shift. The first 10% of posterior samples were discarded as burn-in. All parameter estimates have effective

sample sizes well over 200. Two independent chains were run per analysis to verify MCMC convergence. We analyzed our data under three model settings: the *Paleobiome* setting that used the time-heterogeneous graphical structure presented in Figure 2; the *Modern Biome* setting that used the graphical structure from the Recent time interval to represent all time intervals; and the *Null Biome* setting that ignored regional and biome structure by fixing $w_U = 1$.

Departing from the general model description above, we reparameterized our applied model to eliminate informative priors wherever possible. This helped ensure that our posterior estimates are driven by the data through the likelihood function, not the prior (discussed further in Supplement 2). We assigned uninformative prior distributions to our graph weights, $(w_U, w_L, w_B) \sim \text{Dirichlet}(1, 1, 1)$, and to our weak feature strength parameter, $y \sim \text{Uniform}(0, 1)$. We treated each biome shift rate as an independently estimated parameter, $\beta_{i,j} \sim \text{Uniform}(0, 1)$, although we fixed the biome shift rates between tropical and cold temperate biomes equal to zero. Fixing those transition rates to zero both reduces the number of free parameters and reflects the observation that, analogous to the geographical structure of regions, biomes have an important ecological and climatological structure (Whittaker 1970). In *Viburnum*, this assumption is reasonable, as the clade contains no tropical-cold temperate sister species pairs, and previous ancestral biome estimates for the group did not confidently infer any shifts between those biomes (Landis et al. 2019). Because we constrained biome-independent dispersal between regions through graphical structures (Q_G) and weight parameters (w_U and w_G), we fixed the relative dispersal rate to $\delta_{k,l} = 1$ (which is potentially rescaled by Q_G and w_G). Thus, the relative biome shift rates β and dispersal rates δ all have values between 0 and 1. To model

488 the relative proportion of biome shifts to dispersal events, we multiply β by the factor $f_\beta \sim$
489 Uniform(0,1) and multiply δ by $f_\delta = (1 - f_\beta)$. Finally, we rescaled the instantaneous rate
490 matrix, Q, for the entire evolutionary process by a global clock parameter, $\mu \sim$
491 LogUniform$(10^{-4}, 10^{1})$, that is uniformly distributed over orders of magnitude. For the
492 *Viburnum* analysis, we used Bayes factors (Jeffreys 1935) to compare the relative fit of the
493 *Paleobiome*, *Modern Biome*, and *Null Biome* models to the data. Power-posterior
494 distributions were approximated with a parallelized MCMC sampler (Höhna et al. 2017).
495 Marginal likelihoods were estimated from those power-posterior samples using the
496 stepping stone algorithm (Xie et al. 2011).
497 Our analysis produced several inferences, which we summarized in various ways.
498 Ancestral states and stochastic mappings (Huelsenbeck et al. 2003) were generated during
499 MCMC sampling by first drawing ancestral state estimates for all nodes in phylogeny, then
500 sampling evolutionary histories using a uniformization method (Rodrigue et al. 2008) that
501 was adapted for time-stratified models (Landis et al. 2017). Ancestral state estimates show
502 the posterior probabilities for biome-region states for each node. Lineage-state proportions
503 through time were computed from the posterior distributions of stochastically mapped
504 histories. We computed the posterior mean count of lineage-states through time as the
505 number of lineages in each state for each time bin across posterior samples divided by the
506 total number of posterior samples. Lineage-state counts were converted into lineage-state
507 proportions by dividing each count by the total number of lineages in that time bin to give
508 proportions that lie between 0 and 1. In addition, we classified whether or not each
509 lineage-state for each time bin was congruent with any locally prominent biome as defined
510 by the paleobiome graph (Fig. 2). Each binned state was labeled as a *biome mismatch* if the

lineage's biome had only a marginal presence in the lineage's region. Otherwise, the state was labelled as a *biome match*. To summarize these results, we also computed the proportion of tree length where lineage states match or mismatch paleobiome structure in three ways: for the total tree length, for tree length before the Oligocene (>34 Ma), and for tree length after the Oligocene (≤ 34 Ma). To assess whether the use of the *Paleobiome* model unduly biased posterior estimates (e.g. by inflating the prior expectations of biome match proportions), we generated stochastic mappings conditional on the phylogeny and tip states while sampling model parameters from the prior (details given in Supplement 2).

We were also interested in the ordered *event series* that resulted in major transitions between biomes and regions. For biomes A, B, and C and regions X, Y, and Z, we named the six series patterns for pairs of events. Series in which species shift biomes and then disperse ($AX \rightarrow BX \rightarrow BY$) are called *biome-first* event series. In contrast, *region-first* series have dispersal followed by a biome shift event ($AX \rightarrow AY \rightarrow BY$). The remaining four event series involve two consecutive biome shift or two dispersal events. *Biome reversal* ($AX \rightarrow BX \rightarrow AX$) and *region reversal* ($AX \rightarrow AY \rightarrow AX$) sequences indicate event series in which the lineage departs from and then returns to its initial state (AX). Analogously, *biome flight* ($AX \rightarrow BX \rightarrow CX$) and *region flight* ($AX \rightarrow AY \rightarrow AZ$) sequences are recognized by series of two biome shifts or two dispersal events that leave the lineage in a new state (CX or AZ) relative to the lineage's initial state (AX). We computed the proportion of each series type for a single posterior sample by classifying stochastically mapped state triplets (event series of length two) in our phylogenetic tree using a simple root-to-tip recursion. To start the recursion, we took the stochastically mapped root state to be the second state

in the triplet, X_{root}, then sampling the preceding state, X_{subroot}, from the sampling distribution obtained by Bayes rule

$$P(X_{\text{subroot}} = (i,k) \mid X_{\text{root}} = (j,l), Q(m_{\text{root}})) \propto \frac{[Q(m_{\text{root}})]_{(i,k),(j,l)}}{\sum_{(x,y)\neq(i,k)} [Q(m_{\text{root}})]_{(i,k),(x,y)}} \times \frac{[\pi(m_{\text{root}})]_{(i,k)}}{[\pi(m_{\text{root}})]_{(j,l)}}$$

where $Q(m_{\text{root}})$ is the root node's rate matrix and $\pi(m_{\text{root}})$ is its stationary distribution with values determined by the evaluated posterior sample. Following that, we traversed towards the tips of the tree to collect changes in the stochastic mapping for each lineage's biome-region state, classifying the state triplet's type, and updating the triplet states appropriately (i.e. the new second and third states replace the old first and second states) with each step of the recursion.

Finally, we wished to examine if and how the distribution of evolutionary events and event series changed with time under alternative assumptions about the biome structure. We were particularly interested in two classes of event proportions: proportions of various types of biome shift and dispersal events, and proportions of the various types of event series. To estimate the posterior proportions of biome shift and dispersal event types through time, for each posterior sample, we divided the count for each distinct biome shift and dispersal event type by the total number of events within each major time interval. Event proportions from the Late Cretaceous could not be reliably estimated, as the two *Viburnum* lineages that existed between the origin of the group (~70 Ma) and the end of the Late Cretaceous (~66 Ma) rarely changed in biome-region state. Although we normalized our event proportions using all 126 distinct dispersal and biome shift event types, our results only display the four biome shift and four dispersal event types among all combinations of the warm and cold temperate forests of East Asia and North America. In a

similar manner, we computed the posterior proportions for all six types of event series, using the time of the second event in each series for each series age.

We provide the posterior means and the 80% and 95% highest posterior densities (HPD80 and HPD95, respectively) for each time interval, event or event series type, and biome structure model. Constructing Bayesian credible intervals for these proportions is somewhat unusual, since the proportions are ratios of counts (i.e. not all numbers on the real line are supported). As a result, several HPDs share the exact same bounds, particularly when the total number of events is low (e.g. values such as 1/2 or 1/3).

Simulation experiment

We measured how reliably we can select models in which biome structure influences the biome shift process ($w_B > 0$) for *Viburnum* with simulated data. All simulations assumed the same *Viburnum* phylogeny used in the empirical example and used the same biome and regions designated by the paleobiome structure model. We simulated data under five conditions that primarily adjusted the relative weight for w_B, named: null effect, where $(w_U, w_G, w_B) = (1,0,0)$; weak effect, where $(w_U, w_G, w_B) = (1,2,4)/7$; medium effect, where $(w_U, w_G, w_B) = (1,2,8)/11$; strong effect, where $(w_U, w_G, w_B) = (1,2,16)/19$; and very strong effect, where $(w_U, w_G, w_B) = (1,2,32)/35$; with each denominator ensuring the weights sum to 1. For all conditions, we assumed $f_\beta = 0.75$, $f_\delta = 0.25$, and $y = 0.1$. Biome shift rates were set to equal 1, except transitions between cold temperate and tropical forests, which were set to 0. The event clock was set to $\mu = 0.03$, except for the null condition, which was assigned a slower rate of $\mu = 0.01$ to account for the fact that fewer event rate penalties are applied to it than the non-null conditions.

We then simulated 100 replicate datasets in RevBayes for each of the four conditions under the regional biome-shift model described above, and estimated the posterior density for each simulated dataset using MCMC in RevBayes.

We were primarily concerned with how our posterior estimates of w_B respond to differing simulated values for w_B. To summarize this, we first report the posterior median values of w_B across replicates so they may be compared to the true simulating value. Next, we computed what proportion of our replicates select a complex model allowing $w_B > 0$ in favor of a simpler model where $w_B = 0$ using Bayes factors. Bayes factors were computed using the Savage-Dickey ratio (Verdinelli and Wasserman 1995), defined as the ratio of the prior probability divided by the posterior probability, evaluated at the point where the complex model collapses into the simpler model (i.e. $w_B = 0$, in our case). We approximated the posterior probability at this collapse-point by smoothing our posterior samples for w_B with a beta-kernel density estimator (Moss and Tveten, 2019). We interpret the strength of significance for Bayes factors as proposed by Jeffreys (1961), requiring at least 'Substantial' support (BF > 3) to select the more complex model ($w_B > 0$).

RESULTS

Simulation experiment

Simulated datasets yielded larger estimates of w_B and more soundly rejected null models ($w_B = 0$) as the effect strength w_B increased from Weak to Very Strong (Fig. 4). No datasets simulated under the Null condition ($w_B = 0$) signalled Substantial support (or greater) for the paleobiome-dependent model ($w_B > 0$), indicating a low false positive rate. Only 9% of datasets simulated under Weak effects ($w_B = 4/7 \approx 0.57$) generated No

support for the $w_B > 0$ model, while ~32% of those replicates qualified as Substantial support or greater. Data simulated under the Moderate condition ($w_B = 8/11 \approx 0.73$) rejected the simple model 57% of the time with at least Substantial support. Under Strong ($w_B = 16/19 \approx 0.84$) simulation conditions, we selected models where $w_B > 0$ in 81% of cases, with Strong support in 65% of cases. Data simulated under Very Strong effects ($w_B = 32/35 \approx 0.91$) generated support for models with $w_B > 0$ 88% of the time, with over half of all replicates (54%) drawing Very Strong or Decisive support. Coverage frequency among simulations was consistently high across conditions, but with fairly wide credible intervals corresponding to the highest 95% posterior density (Fig. 4A). Because the posterior probability of $w_B = 0$ is used to approximate Bayes factor ratios, their relationship is made apparent by noting that the density of HPD95 lower bound estimates close to the value $w_B = 0$ (Fig. 4A) is correlated with the proportion of simulations that award no support to the $w_B > 0$ model (Fig. 4B).

Ancestral biomes for Viburnum

Although *Viburnum* likely originated in East Asia regardless of the biome structure model ($p > 0.99$), no model reconstructed a single ancestral biome affinity with probability greater than $p > 0.95$ (Fig. 5). Where the *Paleobiome* analysis inferred East Asian biome affinities that favored a warm temperate ($p = 0.88$) or tropical ($p = 0.09$) but not a cold temperate ($p = 0.03$) origin, the *Modern Biome* analysis favored a cold temperate ($p = 0.67$) then warm temperate ($p = 0.31$) origin for *Viburnum* while assigning negligible probability to a tropical origin ($p = 0.01$). Relative to the *Paleobiome* estimates, the *Null Biome* analysis also assigned higher probabilities to colder biomes (warm, $p = 0.52$; cold,

624 $p = 0.45$; tropical, $p = 0.02$). Early diverging *Viburnum* lineages tended to follow
625 warm/tropical biome affinities under the *Paleobiome* analysis or the cold/warm affinities
626 under the *Modern*/*Null Biome* analyses before the Oligocene (>34 Ma). During the
627 Oligocene (34–22 Ma), when cold temperate forests first expanded, many nodes still
628 retained the warmer (*Paleobiome*) or colder (*Modern Biome*) affinities characteristic of the
629 biome structure model, such as the most recent common ancestor (MRCA) of *V. reticulatum*
630 and *V. ellipticum* or the MRCA of *V. rufidulum* and *V. cassinoides*. Otherwise, most ancestral
631 biome inferences were consistent across the three models, beginning with the Mid/Late
632 Miocene (<16 Ma).
633 The three biome structures recovered different proportions of ancestral lineage-
634 states through time, particularly before the Mid/Late Miocene (>16 Ma; Fig. 6A–C).
635 Between the Paleocene and the Early Miocene, tropical lineages in East Asia and Southeast
636 Asia constituted >20% diversity, declining to ~12% of modern diversity under the
637 *Paleobiome* analysis. Cold temperate lineages were nearly absent until the end of the
638 Oligocene (34 Ma), but steadily rose to constitute roughly 25% of diversity by the
639 Early/Mid Miocene (ca. 20 Ma). By comparison, *Modern Biome* estimates enriched the
640 proportion of cold temperate viburnums, while reducing support for warm temperate and
641 nearly eliminating support for tropical origins; tropical lineages remained in comparatively
642 low proportion until the Miocene (< 22 Ma). The *Null Biome* analysis estimated
643 proportions of warm and cold temperate lineages similar to those of the *Modern Biome*
644 analysis from the Late Cretaceous (100 Ma) until the Oligocene (34 Ma), but with more
645 Southeast Asian warm temperate lineages throughout.

For what proportion of time did lineages have biome affinities that were congruent with locally accessible biomes? Biomes rarely mismatched between lineages and regions under the *Paleobiome* setting (1.1% of tree length), with the mismatches increasing under the *Modern Biome* (8.6%) and *Null Biome* (8.7%) settings. Lineages were most often mismatched with their regions' biomes before the Oligocene (Figs. 6D–F), where the pre-Oligocene proportion of mismatched branch lengths was always higher (*Paleobiome*, 5.8%; *Modern Biome*, 52.6%; *Null Biome*, 47.1%) than the post-Oligocene proportion (*Paleobiome*, 0.3%; *Modern Biome*, 0.8%; *Null Biome*, 1.7%) or the treewide proportions (above). The prior distributions of stochastic mappings that we generated under the *Paleobiome*, *Modern Biome*, and *Null Biome* settings were nearly indistinguishable from one another (Supplement 2; Fig S1). It is therefore unlikely that our posterior inferences are artifacts caused by undesirable interactions between our prior model and our biome structure models.

To illuminate why the *Paleobiome* analysis produces distinctly warmer ancestral biome estimates, we turn to the fitted stationary probability for the root state, $\pi(m_{\text{root}})$, (Fig. 7). Within East Asia, root node stationary probabilities estimated under the *Paleobiome* setting favored warm temperate or tropical forests over cold temperate forests ($\pi_{\text{Trop+EAs}} = 0.06, \pi_{\text{Warm+EAs}} = 0.10, \pi_{\text{Cold+EAs}} = 0.02$). The *Modern Biome* stationary probabilities instead favored cold or warm temperate forests over tropical forests ($\pi_{\text{Trop+EAs}} = 0.03, \pi_{\text{Warm+EAs}} = 0.07, \pi_{\text{Cold+EAs}} = 0.08$). Like the *Modern Biome* analysis, stationary probabilities under the *Null Biome* setting tended towards cold or warm temperate forests. ($\pi_{\text{Trop+EAs}} = 0.04, \pi_{\text{Warm+EAs}} = 0.06, \pi_{\text{Cold+EAs}} = 0.06$), noting that the stationary probability per biome is uniform across regions by the design of the model.

While the posterior root node stationary probabilities varied across biome-regions depending on what biome structure model was assumed (Fig. 7), all corresponding prior probabilities are approximately equal (Supplement 2; Fig. S2), suggesting that any differences in the posterior estimates are driven by the data through the likelihood function, and not forced through an induced prior.

Despite such differences between the *Paleobiome* and *Modern Biome* analyses in their ancestral state estimates and stationary probabilities, their parameter estimates for the base rate of change (μ), the proportion of biome shifts (f_β) to dispersal events (f_δ), and the graph weights (w_U, w_G, w_B) were remarkably similar (Table 1). Both biome structure models estimate posterior means for w_B greater than 0.91; i.e., stronger in effect than assumed under the Very Strong simulation scenario (Fig. 4). Both models estimated credible intervals for w_B with lower bounds greater than 0.75 and posterior probabilities of $w_B = 0$ that were indistinguishable from zero, each corresponding to Decisive support for their respective biome structure models. More accurate Bayes factors estimated using marginal likelihoods unequivocally selected either the *Paleobiome* ($BF_{PN} > 10^6$) or the *Modern Biome* ($BF_{MN} > 10^6$) over the *Null Biome* structures for modeling biome shifts in *Viburnum*, but found only mild support in favor of the *Paleobiome* over the *Modern Biome* structure ($BF_{PM} \approx 1.8$). Because inference under the *Null Biome* model set $y = 1$, posterior estimates of (w_U, w_G, w_B) are indistinguishable from the prior. Parameter estimates for the relative biome shift rates differed across the three biome structure models, however. The *Paleobiome* estimates favor hot-to-cold shifts ($\beta_{TW} = 0.63 > \beta_{WT} = 0.43$ and $\beta_{WC} = 0.82 > \beta_{CW} = 0.29$) while the *Modern Biome* estimates favor shifts leaving the warm temperate

biome ($\beta_{TW} = 0.44 < \beta_{WT} = 0.65$ and $\beta_{WC} = 0.80 > \beta_{CW} = 0.42$), as do the *Null Biome* estimates ($\beta_{TW} = 0.55 < \beta_{WT} = 0.76$ and $\beta_{WC} = 0.73 > \beta_{CW} = 0.32$).

Finally, we found that the *Paleobiome* analysis estimated proportions of biome shift and dispersal events that are more temporally dynamic than those proportions estimated under the *Modern Biome* and *Null Biome* models (Fig. 8A–C). Under the *Paleobiome* estimates, dispersal events from East Asia into North America within the warm temperate biome were relatively common throughout the Late Eocene. With the onset of Oligocene cooling, biome shifts from warm into cold temperate forests in East Asia rose from low to high proportions to become the most frequent transition type. In contrast, event proportions under the *Modern Biome* and *Null Biome* analyses reconstructed high proportions of biome shifts between the warm and cold temperate forests of East Asia, ever since *Viburnum* first originated in the Late Cretaceous through the present. Paleocene dispersal of cold temperate lineages from East Asia into North America was also found to be relatively common when compared to the *Paleobiome* reconstruction. Regarding the event series proportions, biome reversal, biome-first, and region-first series were generally more common than biome flight, region flight, and region reversal series (Fig. 8D–F). The biome reversal event series was the most common event series type across all time intervals under the *Modern Biome* and *Null Biome* analyses, but not under the *Paleobiome* analysis. With the *Paleobiome* model, we found that the proportion of biome reversal series was lower, and the proportion of region-first series was higher, when compared to the other biome structure analyses, together creating a time interval between the Late Eocene and the Middle Miocene during which region-first events outpaced all other types of series.

DISCUSSION

The probability that a lineage will shift into a new biome is determined in part by geographical opportunities. Because the availability and connectivity of biomes varies across regions, evolutionary lineages do not share the same geographical opportunities to adapt to new biomes. Moreover, those geographical opportunities have changed as the spatial structure of Earth's biomes evolved over time. As an evolutionary inference problem, the temporal dynamics of geographical opportunity is concerning: we typically infer ancestral biomes based on the phylogenetic distribution of biomes from extant species, yet their ancestors were likely exposed to geographical opportunities significantly (perhaps even radically) different from the opportunities of their living descendants. Here, we have developed a Bayesian framework to model how phylogenetic lineages gain affinities with new biomes and disperse between regions in a manner reflecting the historical configuration of biomes through space and time. To do so, we modeled a time-stratified regional biome shift process using continuous-time Markov chains. The model is parameterized to allow biome shift and dispersal rates to depend on empirically structured paleobiome graphs, where each graph describes the availability and connectivity of biomes among regions within a given time stratum. We conducted a simple simulation experiment to show that we can identify which comparative datasets were shaped by paleobiome structure ($w_B > 0$) using Bayes factors, provided the strength of the effect was at least moderately strong, even though w_B is difficult to estimate precisely (Fig. 4). We then fitted our new model to estimate ancestral biomes and regions for *Viburnum*. In discussing our results, we focus on two principal aspects of our study: first, our empirical findings in *Viburnum* and how these may inform other studies seeking to estimate ancestral biomes or

737 regions; and, second, an examination of the model's assumptions and properties, and how
738 the model's realism may be improved in future work.
739
740 *Biome shifts in Viburnum*
741 *Viburnum* first diversified in the Paleocene and Eocene (66–34Ma), a period when
742 boreotropical forests dominated and connected the northern continents (Wolfe 1985;
743 Graham 2011; Willis and McElwain 2014). Cold temperate forests that experienced long
744 freezing periods were globally rare until after the Oligocene (<34 Ma). Although we
745 inferred an East Asian origin regardless of what biome structure model was assumed,
746 ancestral biome estimates under the three structure models differed in important ways. In
747 the *Paleobiome* analysis, the ancestral biome of the crown node was probably warm
748 temperate ($p = 0.88$) and possibly tropical ($p = 0.09$), and a cold temperate origin could
749 decisively be ruled out ($p < 0.05$; Fig. 5A). When we assumed that biome structure had
750 always resembled today's structure (*Modern Biome*), the crown node support changed,
751 instead favoring a cold temperate ($p = 0.67$) or possibly a warm temperate ($p = 0.31$)
752 origin (Fig. 5B). The *Null Biome* reconstruction also recovered a warm ($p = 0.52$) or cold
753 ($p = 0.45$) temperate origin, despite the fact that the *Null Biome* inference assumed that all
754 biomes are present in all regions at all times (Fig. 5C). Mismatches between lineage biome
755 affinities and regionally available biomes were highest among pre-Oligocene lineages (>34
756 Ma). Though cold temperate lineages remained in low proportions (~5%) until the
757 Oligocene under the *Paleobiome* analysis (Fig. 6A), the *Modern/Null Biome* analyses
758 maintained high proportions of cold temperate lineages in East Asia (> 30%) and North
759 America (7%) in the Eocene (Fig. 6B,C). Over 53% and 47% of pre-Oligocene branches bore

760 mismatched biomes under the *Modern* and *Null Biome* analyses, respectively, but only 6%
761 of those branch lengths were mismatched with biomes under the *Paleobiome* model (Fig.
762 6D–F). Because of the global rarity of the cold temperate biome during the period of early
763 *Viburnum* evolution, we favored the warm temperate or tropical origin of *Viburnum* under
764 the *Paleobiome* analysis.

765 Yet, despite stark differences in the *Paleobiome* and *Modern Biome* models,
766 parameter estimates under both conditions found the spatial distribution of biomes to be
767 the primary factor in explaining how viburnums came to live where they do today ($w_B >$
768 0.92, i.e. compatible with the Very Strong condition used in the simulation experiment).
769 Because the ability to estimate ancestral states or to fit evolutionary parameters decays as
770 the evolutionary timescale deepens, we expect that both the *Paleobiome* and *Modern Biome*
771 analyses primarily fit their parameters to phylogenetic patterns of variation pronounced at
772 the shallowest timescales. True to this, model selection by Bayes factors only slightly
773 prefers the *Paleobiome* over the *Modern Biome* structure. All else being equal, however,
774 older *Viburnum* lineages should disperse and biome shift in a manner that is similarly
775 limited by geographical opportunities. The static geographical opportunities assumed
776 under the *Modern Biome* structure induced stationary probabilities that project today's
777 colder conditions back into the Late Cretaceous, while the dynamic *Paleobiome* structure
778 favored hotter conditions unlike those at present (Figs. 2 and 7). The lesson we take from
779 this is that inferring the fundamental behavior of the process is not always sufficient for
780 estimating ancestral states; inferring if and how that behavior responds to changing
781 historical conditions is also necessary.

We note that an East Asian origin in warm temperate or tropical forests is consistent with several other relevant lines of evidence developed in the study of *Viburnum* evolution, biogeography, and ecology. Previous efforts to reconstruct the ancestral biome of *Viburnum* have weakly favored warm temperate (Spriggs et al. 2015) or cold temperate (Lens et al. 2016) conditions; neither study definitively supported or ruled out a cold temperate origin. Similarly, Edwards et al. (2017) established a relationship between cold temperate conditions and the evolution of deciduousness in *Viburnum*, but could not resolve whether the MRCA was deciduous (cold-adapted) or evergreen (tropical or warm-adapted). Landis et al. (2019) estimated a warm temperate origin of *Viburnum*, with no support for a cold temperate origin, through a combined-evidence tip-dating analysis (Ronquist et al. 2012) that included fossil pollen coded with biome characters to inform the ancestral biome estimates. As a fossil-based estimate, the finding of a non-freezing origin of *Viburnum* cannot be accepted unconditionally; the estimate depends crucially upon the accuracy of biome state assignments to the fossil taxa, and also upon the spatial and temporal biases inherent to fossil deposition and recovery. But, importantly, the fossil-aware biome estimates of Landis et al. (2019) were obtained under the equivalent of our *Null Biome* model, while the fossil-naive estimates in the present study were obtained under the *Paleobiome* model. It is highly satisfying that both studies rule out a cold temperate ancestry for *Viburnum*, and that they do so by leveraging alternative lines of paleobiological evidence: the phylogenetic placement of fossils assigned to particular biomes in one case, and the inferred spatial distribution of biomes through time in the other.

Examining only extant *Viburnum* species, the clade displays considerable variation in both which biomes and which regions lineages occupy. Yet, each region does not contain

equal proportions of lineages with affinities to the three biomes. There are several possible causes for this imbalance. In many cases, lineages may simply inhabit regions that lack certain biomes; it is not surprising that there are no extant tropical lineages in North America given that tropical forests have been marginal there since the Oligocene. In other cases, lineages may not have had long enough periods of time for certain biome shifts. For example, all neotropical lineages are adapted to warm temperate (cloud) forests, yet none of them have adapted to the adjacent tropical forest biome. Given the young age of the neotropical radiation, it is possible that there has not been enough time for them to shift into the accessible tropical forests. In this case we can imagine that biological factors (e.g., interactions with other species—competitors, herbivores, etc.—that have long occupied tropical forests) may have played a significant role in limiting this shift (Donoghue and Edwards 2014). In other cases, the imbalance may concern differential rates of speciation or extinction within biomes. For instance, there are relatively few tropical *Viburnum* species given the age and region of origin for the clade and given the age of Asian tropical biomes. If tropical viburnums experienced increased extinction rates (or decreased speciation rates) as they remained in an older biome, that effect would give rise to a pattern of scattered, singular, distantly related, and anciently diverging tropical lineages (depauperons of Donoghue and Sanderson 2015). This is precisely what we see in the case of *V. clemensiae*, *V. amplificatum*, and *V. punctatum* (Spriggs et al. 2015). From analyses under our simple *Paleobiome* model, it appears that temporal, geographical, and ecological influences on rates of character evolution and lineage diversification may all be important factors in explaining why *Viburnum* is distributed as it is across regions and biomes.

827 Finally, although we question the general validity (often assumed) of stepwise series
828 of events (e.g., trait-first versus climate-first in the evolution of cold tolerance; Edwards et
829 al. 2015), we nevertheless explored how incorporating information on the past distribution
830 of biomes might influence the inference of biome-first versus region-first event series.
831 Specifically, we asked whether *Viburnum* lineages tended to shift biomes first or disperse to
832 a new region first when radiating through the mesic forests of Eurasia and the New World.
833 Taking the mean proportions across time intervals, we found that when *Viburnum* lineages
834 both disperse into new regions and shift into new biomes, region-first event series (28% of
835 series) are more common than biome-first (19%) series under the *Paleobiome* model.
836 Alone, this result is difficult to interpret, since the relative number and size of biome and
837 region states will influence what constitutes a biome shift or dispersal event. Using the
838 *Modern* analysis as a point of reference, we find a comparatively neutral relationship, with
839 roughly equal proportions of biome-first (20%) and region-first (21%) series, while under
840 the *Null Biome* analysis the *Paleobiome* relationship is inverted (biome-first, 22%; region-
841 first, 19%). When all regions contain all biomes (*Null Biome*), it makes sense that the ratio
842 of biome-first to region-first series is highest, and that it decreases when the distribution of
843 biomes is not uniform across regions (*Paleobiome* and *Modern Biome*). In the case of
844 *Viburnum*, it appears that several key regional shifts between Eastern Asia and North
845 America occurred a relatively long time ago, when northern latitudes were still primarily
846 covered by warm temperate forests (Fig. 8A). The biome shifts into cold temperate forests
847 occurred later, as cooling climates spread across communities that were already
848 assembled, which is compatible with the 'lock-step' hypothesis of Edwards et al. (2017).
849 Consistent with this scenario, we found that region-first event series do not become the

most common series type (over 35%) until the Late Oligocene under the *Paleobiome* model (Fig. 8D). Such region-first event series have also been inferred in several recent analyses, most notably by Gagnon et al. (2019) who found that *Caesalpinia* legumes moved frequently among succulent biomes on different continents, and only later shifted into newly encountered biomes within each continent (Donoghue 2019). From our findings, we suspect that ignoring paleobiome structure may cause the number of region-first transition series to be underestimated. However, it must be borne in our minds that our results may in part reflect the constraint built into our model that simultaneous shifts in biome and region are not allowed (discussed below). In any case, explicitly testing for the effect of paleobiome structure on event order will be important in evaluating patterns of supposed phylogenetic biome conservatism (Crisp et al. 2009).

Model discussion

Although our model is simple, it is designed with certain statistical features that would allow the model to be applied to diverse datasets beyond *Viburnum*, and to facilitate extensions of the model towards more sophisticated designs. First, we treat many elements in the evolutionary process as free parameters, whose values we estimate from the phylogenetic dataset in question. For example, the *w* parameters control which layers of the paleobiome graphical structure are most relevant to the evolutionary process, and the *y* parameter controls how important weak structural features are when modeling dispersal or biome shift events. Second, the Bayesian modeling framework we chose is ideal for managing complex and parameter-rich hierarchical models (Höhna et al. 2016), allowing for future models to explore the importance of other factors highlighted in the conceptual

873 model of Donoghue and Edwards (2014) — geographical distance (Webb and Ree 2012),
874 region size (Tagliacollo et al. 2015), biome size and shared perimeter (Cardillo et al. 2017),
875 ecological distance (Meseguer et al. 2015), and the effect of biotic interactions on trait and
876 range evolution (Quintero and Landis 2019) — by introducing new parameterizations for
877 computing the time-stratified rate matrices, $Q(m)$. Our Bayesian framework is also capable
878 of handling sources of uncertainty in the paleobiome graphs, such as uncertainty in the
879 importance of various spatial features or in the age of the appearance of a biome within a
880 region (Landis et al. 2018).

881 In our application of the model to *Viburnum*, we defined only three biomes and six
882 regions, but the general framework translates to other biogeographical systems with
883 different regions and biomes, provided one can construct an adequate time series of
884 paleobiome graphs. Though our literature-based approach to paleobiome graph
885 construction was somewhat subjective, we found it to be the most integrative way to
886 summarize varied global biome reconstructions, as most individual studies are purely
887 qualitative (Wolfe 1985; Morley 2000; Jetz and Fine 2012; Willis and McElwain 2014;
888 Graham 2011; Graham 2018; but see Kaplan et al. 2003) and based on disparate lines of
889 paleoecological, paleoclimatological, and paleogeological evidence. We believe that our
890 paleobiome graphs for the Northern Hemisphere are sufficiently accurate to show that
891 spatial and temporal variation in the distribution of tropical, warm temperate, and cold
892 temperate forest biomes in space and time can influence how species ranges and biome
893 affinities evolve over time. Nonetheless, future studies should explore more quantitative
894 approaches to defining paleobiome structures for use with the time-stratified regional
895 biome shift model.

Our simple model of regional biome shifts lacks several desired features. Perhaps most importantly, lineages in our model may only occupy a single region and a single biome at a time when, in reality species may occupy multiple biomes and/or regions (e.g., *Liquidambar styraciflua* is a tree that thrives both in temperate deciduous forests of eastern North America and in the cloud forests of Mexico). On paper, it is straightforward to extend the concepts of this model to standard multi-character models, such as the Dispersal-Extinction-Cladogenesis model (Ree et al. 2005; Matzke 2014; Sukumaran et al. 2015). As a DEC model variant, lineages would be capable of gaining affinities with any biomes available within their range. For example, for M biomes and N regions, there are on the order of 2^{M+N} combinations of presences and absences across biomes and regions, and on the order of 2^{MN} combinations if region-specific biome occupancies are considered. Computationally, this creates a vast number of viable state combinations, many of which cannot be eliminated from the state space (Webb and Ree 2012). Such a large state space will hinder standard likelihood-based inference procedures for discrete biogeography (Ree and Sanmartín 2009), though recent methodological advances addressing this problem should prove useful (Landis et al. 2013; Quintero and Landis 2019).

Geographical state-dependent diversification (GeoSSE) models may also be interfaced with our model. Incorporating the effect of biome availability on the extinction rate would, at a minimum, be a very important contribution towards explaining patterns of extant diversity. For example, tropical biomes have declined in dominance since the Paleogene, and many ancient *Viburnum* lineages may have since gone extinct in the tropics, perhaps owing to biotic interactions (the dying embers hypothesis of Spriggs et al. 2015). In this sense, we expect that our model will overestimate how long a lineage may persist in

919 a region that lacks the appropriate biome, since our model does not threaten ill-adapted
920 species with higher extinction rates. Efforts to extend GeoSSE models in this manner will
921 face similar, if not more severe, challenges to those encountered in the DEC framework,
922 both in terms of computational limits and numbers of parameters (Beaulieu and O'Meara
923 2016; Caetano et al. 2018).

924 If diversification rates vary conditionally on a lineage's biome-region state, then so
925 should the underlying divergence time estimates. At a minimum, one should jointly
926 estimate divergence times and diversification dynamics to correctly propagate uncertainty
927 in phylogenetic estimates through to ancestral state estimates (Höhna et al. 2019). Beyond
928 that, paleogeographically structured models of biogeography have been shown to be useful
929 for estimating divergence times (Landis 2017; Landis et al. 2018). Paleoecological models,
930 such as our *Paleobiome* model, could be useful in some cases, perhaps for dating clades
931 where some degree of phylogenetic niche conservatism can be safely assumed (Wiens and
932 Donoghue (2004); Crisp et al. (2009); but see Donoghue and Edwards (2014) for potential
933 pitfalls with this approach). For instance, Baldwin and Sanderson (1998) hypothesized that
934 continental tarweeds (*Madiinae*, Asteraceae) radiated within the seasonally dry California
935 Florisitic Province only after Miocene aridification created the province. Baldwin and
936 Sanderson (1998) translated this relationship between biome age and biome affinity to
937 date the maximum crown age of tarweeds, and thus date the maximum crown age of a
938 notable radiation nested within the tarweeds, the Hawaiian silversword alliance. In the
939 future, rather than calibrating the age of tarweeds by asserting a paleoecological
940 hypothesis, it would be possible to use our biome shift model to measure the probability of
941 the dry radiation scenario against competing scenarios, thereby dating the tarweeds (or

942 other clades) based on what ecological opportunities they made use of in different areas
943 and at different times (Baldwin and Sanderson 1998; Landis 2017; Landis et al. 2018).
944 Finally, although we have compared inferences of event series under several biome
945 structure models, and have argued that paleobiome models can influence such inferences,
946 we caution that event series themselves may not be accurate descriptors of some relevant
947 evolutionary scenarios. Notably, we reiterate that our model does not allow for
948 simultaneous shifts in both biome and biogeographic region. In other words, all biome
949 shifts are restricted to occur within a biogeographic region. This makes several important
950 assumptions about the processes involved in biome shifting. The first is that movements
951 between biomes are non-trivial for organisms, and require a period of time that allows a
952 founding population to adapt to its new environment. If this is true, we see two scenarios
953 that would likely describe the vast majority of biome shifts. First, if two biomes are
954 adjacent to one another, repeated propagule dispersal from the ancestral to the novel
955 biome could allow for gradual adaptation to a new habitat. Second, biome shifts could occur
956 "in-situ", as one major vegetation type gradually transforms into another, in place, as
957 climate change progresses ("lock-step" model of Edwards et al. 2017). Both of these
958 scenarios would occur *within* biogeographical regions, and we think they probably have
959 accounted for biome shifts in *Viburnum*, as well as many other lineages. However, it is also
960 possible that a shift into a new biome could occur *during* a transition from one region into
961 another. For example, a lineage might adapt to colder forests during range expansion
962 through Beringia, or there might be long-distance dispersal of an organism already pre-
963 adapted to occupy a novel biome. Furthermore, it is important to note that our restriction
964 of biome shifts to occur within biogeographical regions does not completely preclude long-

965 distance dispersal biome shifts within regions; nothing in our model ensures that ancestral
966 and novel biomes are adjacent to one another within a given region, especially given that
967 the regions often used are very large and environmentally heterogeneous. Such
968 considerations highlight that the model we have presented here is simplistic in some of its
969 basic assumptions. We view it as a start in the right direction, and look forward to
970 extensions that will allow us to test a variety of more nuanced hypotheses.

971

972 ## CONCLUSION

973 The potential for a lineage to adapt to new biomes depends in part on the
974 geographical opportunities that the lineage encountered in time and space. In the case of
975 *Viburnum*, we have shown that differing assumptions about the past distribution of biomes
976 can have a significant impact on ancestral biome estimates. And, when we integrate
977 information about the changing distribution of biomes through time, we favor an origin of
978 *Viburnum* in warm temperate or tropical forests, and confidently rule out an origin in cold
979 temperate forests. The confluence of this line of evidence with our analyses based instead
980 on fossil biome assignments (Landis et al. 2019) provides much greater confidence in a
981 result that orients our entire understanding of the direction of evolution and ecological
982 diversification in this clade.

983 More generally, we hope that our analyses will motivate biogeographers who wish
984 to estimate ancestral biomes to account for variation in the spatial distribution of biomes
985 through time. We also caution that phylogenetic estimates of ancestral biome affinities that
986 derive entirely from extant taxa and biomes may be misleading, particularly for older
987 lineages, even when standard statistical diagnostics indicate that the inference model fits

988 the data well. While we have achieved some conceptual understanding of the interplay
989 between biome shifts in lineages and biome distributions over time, many theoretical and
990 statistical problems must still be solved for us to fully appreciate the significance of
991 changing biome availability in generating Earth's biodiversity. In presenting our simple
992 model, we hope to provoke further inquiry into how life diversified throughout the biomes
993 of an ever-changing planet.
994

995 ## FUNDING

996 This work was supported by the NSF Postdoctoral Fellowship (DBI-1612153) to MJL
997 and a Gaylord Donnelley Environmental Fellowship to MJL through the Yale Institute of
998 Biospheric Studies. Our research on *Viburnum* has been funded through a series of NSF
999 awards to MJD and EJE (most recently, DEB-1557059 and DEB-1753504), and in part
1000 through the Division of Botany of the Yale Peabody Museum of Natural History.
1001

1002 ## ACKNOWLEDGEMENTS

1003 We thank Bryan Carstens, Mark Holder, and two anonymous reviewers for their
1004 thoughtful comments. Ignacio Quintero, Nate Upham, David Polly, and Tracy Heath
1005 provided useful feedback that helped us frame the context of the research. We also wish to
1006 thank Paul Valdes, who provided us with various BIOME4 reconstructions. Finally, we
1007 express gratitude to the Donoghue, Edwards, and Near lab groups for supporting the
1008 development of this work since its inception.
1009

REFERENCES

Baldwin, B. G., and M. J. Sanderson. 1998. Age and rate of diversification of the Hawaiian silversword alliance (Compositae). *Proceedings of the National Academy of Sciences* 95: 9402–6.

Baskin, J. M. and C. C. Baskin. 2016. Origins and Relationships of the Mixed Mesophytic Forest of Oregon–Idaho, China, and Kentucky: Review and Synthesis. *Ann. Missouri Bot. Gard.* 101: 525-552.

Beaulieu, J. M., and B. C. O'Meara. 2016. Detecting Hidden Diversification Shifts in Models of Trait-Dependent Speciation and Extinction. *Systematic Biology* 65: 583–601.

Bielejec, F., P. Lemey, G. Baele, A. Rambaut, and M. A. Suchard. 2014. Inferring Heterogeneous Evolutionary Processes Through Time: From Sequence Substitution to Phylogeography. *Systematic Biology* 63: 493–504.

Buerki, S., F. Forest, N. Alvarez, J. A. A. Nylander, N. Arrigo, and I. Sanmartín. 2011. An Evaluation of New Parsimony-Based Versus Parametric Inference Methods in Biogeography: A Case Study Using the Globally Distributed Plant Family Sapindaceae. *Journal of Biogeography* 38: 531–50.

Caetano, D. S., B. C. O'Meara, and J. M. Beaulieu. 2018. Hidden State Models Improve State-Dependent Diversification Approaches, Including Biogeographical Models. *Evolution* 72: 2308–24.

Cardillo, M., P. H. Weston, Z. K. M. Reynolds, P. M. Olde, A. R. Mast, E. M. Lemmon, A. R. Lemmon, and L. Bromham. 2017. The phylogeny and biogeography of *Hakea* (Proteaceae) reveals the role of biome shifts in a continental plant radiation. *Evolution* 71: 1928–43.

1033 Chatelet, D. S., W. L. Clement, L. Sack, M. J. Donoghue, and E. J. Edwards. 2013. The Evolution
1034 of Photosynthetic Anatomy in *Viburnum* (Adoxaceae). *International Journal of Plant*
1035 *Sciences* 174: 1277–91.
1036 Clement, W. L., M. Arakaki, P. W. Sweeney, E. J. Edwards, and M. J. Donoghue. 2014. A
1037 Chloroplast Tree for *Viburnum* (Adoxaceae) and Its Implications for Phylogenetic
1038 Classification and Character Evolution. *American Journal of Botany* 101: 1029–49.
1039 Crisp, M. D., M. T. K. Arroyo, L. G. Cook, M. A. Gandolfo, G. J. Jordan, M. S. McGlone, P. H.
1040 Weston, M. Westoby, P. Wilf, and P. H. Linder. 2009. Phylogenetic Biome
1041 Conservatism on a Global Scale. *Nature* 458: 754–56.
1042 Donoghue, M. J. 2008. A Phylogenetic Perspective on the Distribution of Plant Diversity.
1043 *Proceedings of the National Academy of Sciences* 105: 11549–55.
1044 Donoghue, M. J. 2019. Adaptation Meets Dispersal: Legumes in the Land of Succulents. *New*
1045 *Phytologist* 222: 1667–9.
1046 Donoghue, M. J., and E. J. Edwards. 2014. Biome Shifts and Niche Evolution in Plants. *Annual*
1047 *Review of Ecology, Evolution, and Systematics* 45: 547–72.
1048 Donoghue, M. J., and M. J. Sanderson. 2015. Confluence, Synnovation, and Depauperons in
1049 Plant Diversification. *New Phytologist* 207: 260–74.
1050 Eaton, D. A. R., E. L. Spriggs, B. Park, and M. J. Donoghue. 2017. Misconceptions on Missing
1051 Data in RAD-Seq Phylogenetics with a Deep-Scale Example from Flowering Plants.
1052 *Systematic Biology* 66: 399–412.
1053 Edwards, E. J., D. S. Chatelet, B. Chen, J. Y. Ong, S. Tagane, H. Kanemitsu, K. Tagawa, et al.
1054 2017. Convergence, Consilience, and the Evolution of Temperate Deciduous Forests.
1055 *The American Naturalist* 190: S87–S104.

1056 Edwards, E. J., J. M. de Vos, and M. J. Donoghue. 2015. Doubtful Pathways to Cold Tolerance
1057 in Plants. *Nature* 521: E5.
1058 Felsenstein, J. 1981. Evolutionary Trees from DNA Sequences: A Maximum Likelihood
1059 Approach. *Journal of Molecular Evolution* 17: 368–76.
1060 Fine, P. V. A., and R. H. Ree. 2006. Evidence for a Time-Integrated Species-Area Effect on the
1061 Latitudinal Gradient in Tree Diversity. *The American Naturalist* 168: 796–804.
1062 Gagnon, E., J. J. Ringelberg, A. Bruneau, G. P. Lewis, and C. E. Hughes. 2019. Global Succulent
1063 Biome Phylogenetic Conservatism Across the Pantropical Caesalpinia Group
1064 (Leguminosae). *New Phytologist* 222: 1994–2008.
1065 Godfrey, C., M. Fan, G. Jesmok, D. Upadhyay, and A. Tripati. 2018. Petrography and stable
1066 isotope geochemistry of Oligocene-Miocene continental carbonates in south Texas:
1067 Implications for paleoclimate and paleoenvironment near sea-level. *Sedimentary*
1068 *Geology* 367: 69-83.
1069 Goldberg, E. E., K. Roy, R. Lande, and D. Jablonski. 2005. Diversity, endemism, and age
1070 distributions in macroevolutionary sources and sinks. *The American Naturalist* 165:
1071 623–33.
1072 Graham, A. 2011. *A Natural History of the New World: The Ecology and Evolution of Plants in*
1073 *the Americas*. University of Chicago Press.
1074 Graham, A. 2018. *Land Bridges Ancient Environments, Plant Migrations, and New World*
1075 *Connections*. University of Chicago Press.
1076 Heath, T. A., J. P. Huelsenbeck, and T. Stadler. 2014. The Fossilized Birth–Death Process for
1077 Coherent Calibration of Divergence-Time Estimates. *Proceedings of the National*
1078 *Academy of Sciences* 111: E2957–E2966.

1079 Herold, N., J. Buzan, M. Seton, A. Goldner, J. A. M. Green, R. D. Müller, P. Markwick, and M.
1080 Huber. 2014. A suite of early Eocene (~55 Ma) climate model boundary conditions.
1081 *Geoscientific Model Development* 7: 2077–90.
1082 Höhna, S., W. A. Freyman, Z. Nolen, J. P. Huelsenbeck, M. R. May, and B. R. Moore. 2019. A
1083 Bayesian Approach for Estimating Branch-Specific Speciation and Extinction Rates.
1084 *bioRxiv*. https://doi.org/10.1101/555805.
1085 Höhna, S., M. J. Landis, T. A. Heath, B. Boussau, N. Lartillot, B. R. Moore, J. P. Huelsenbeck,
1086 and F. Ronquist. 2016. RevBayes: Bayesian Phylogenetic Inference Using Graphical
1087 Models and Interactive Model-Specification Language. *Systematic Biology* 65: 726–
1088 36.
1089 Höhna, S., M. J. Landis, and J. P. Huelsenbeck. 2017. Parallel power posterior analyses for
1090 fast computation of marginal likelihoods in phylogenetics. *BioRxiv* 104422.
1091 Huelsenbeck, J. P., R. Nielsen, and J. P. Bollback. 2003. Stochastic mapping of morphological
1092 characters. *Syst. Biol.* 52: 131-158.
1093 Jeffreys, H. 1935. Some tests of significance, treated by the theory of probability. *Proc.*
1094 *Camb. Phil. Soc.* 31: 203-222.
1095 Jeffreys, H. 1961. *Theory of Probability*. Oxford: Oxford University Press.
1096 Jetz, W., and P. V. A. Fine. 2012. Global Gradients in Vertebrate Diversity Predicted by
1097 Historical Area-Productivity Dynamics and Contemporary Environment. *PLoS*
1098 *Biology* 10: e1001292.
1099 Kaplan, J. O., N. H. Bigelow, I. C. Prentice, S. P. Harrison, P. J. Bartlein, T. R. Christensen, W.
1100 Cramer, et al. 2003. Climate change and Arctic ecosystems: 2. Modeling, paleodata-

model comparisons, and future projections. *Journal of Geophysical Research: Atmospheres* 108 (D19).

Klaus, K. V., and N. J. Matzke. 2019. Statistical Comparison of Trait-Dependent Biogeographical Models Indicates That Podocarpaceae Dispersal Is Influenced by Both Seed Cone Traits and Geographical Distance. *Systematic Biology* 69: 61–75.

Kosiol, C., I. Holmes, and N. Goldman. 2007. An empirical codon model for protein sequence evolution. *Mol. Biol. Evol.* 24: 1464–1479.

Landis, M. J. 2017. Biogeographic Dating of Speciation Times Using Paleogeographically Informed Processes. *Systematic Biology* 66: 128–44.

Landis, M. J., D. A. R. Eaton, W. L. Clement, B. Park, E. L. Spriggs, P. W. Sweeney, E. J. Edwards, and M. J. Donoghue. 2019. Joint Phylogenetic Estimation of Geographic Movements and Biome Shifts During the Global Diversification of *Viburnum*. *bioRxiv* 832527.

Landis, M. J., W. A. Freyman, and B. G. Baldwin. 2018. Retracing the Hawaiian silversword radiation despite phylogenetic, biogeographic, and paleogeographic uncertainty. *Evolution* 72: 2343–59.

Landis, M. J., N. J. Matzke, B. R. Moore, and J. P. Huelsenbeck. 2013. Bayesian Analysis of Biogeography When the Number of Areas Is Large. *Systematic Biology* 62: 789–804.

Latham, R. E., and R. E. Ricklefs. 1993. Continental Comparisons of Temperate-Zone Tree Species Diversity. *Species Diversity in Ecological Communities: Historical and Geographical Perspectives*, 294–314.

Lens, F., R. A. Vos, G. Charrier, T. van der Niet, V. Merckx, P. Baas, J. Aguirre Gutierrez, et al. 2016. Scalariform-to-Simple Transition in Vessel Perforation Plates Triggered by

1124 Differences in Climate During the Evolution of Adoxaceae. *Annals of Botany* 118:
1125 1043–56.
1126 Lu, L., P. W. Fritsch, N. J. Matzke, H. Wang, K. A. Kron, D. Z. Li, and J. J. Wiens. 2019. Why Is
1127 Fruit Colour so Variable? Phylogenetic Analyses Reveal Relationships Between
1128 Fruit-Colour Evolution, Biogeography and Diversification. *Global Ecology and*
1129 *Biogeography* 28: 891–903.
1130 Matos-Maraví, P., N. J. Matzke, F. J. Larabee, R. M. Clouse, W. C. Wheeler, D. M. Sorger, A. V.
1131 Suarez, and M. Janda. 2018. Taxon Cycle Predictions Supported by Model-Based
1132 Inference in Indo-Pacific Trap-Jaw Ants (Hymenoptera: Formicidae: *Odontomachus)*.
1133 *Molecular Ecology* 27: 4090–4107.
1134 Matzke, N. J. 2014. Model Selection in Historical Biogeography Reveals That Founder-Event
1135 Speciation Is a Crucial Process in Island Clades. *Systematic Biology* 63: 951–70.
1136 Meseguer, A. S., J. M. Lobo, R. Ree, D. J. Beerling, and I. Sanmartín. 2015. Integrating Fossils,
1137 Phylogenies, and Niche Models into Biogeography to Reveal Ancient Evolutionary
1138 History: The Case of *Hypericum* (Hypericaceae). *Systematic Biology* 64: 215–32.
1139 Morley, R. J. 2000. *Origin and Evolution of Tropical Rain Forests.* John Wiley & Sons.
1140 Moss, J. and M. Tveten. 2019. kdensity: An R package for kernel density estimation with
1141 parametric starts and asymmetric kernels. *Journal of Open Source Software* 4: 1566.
1142 Mucina, L. 2019. Biome: Evolution of a Crucial Ecological and Biogeographical Concept. *New*
1143 *Phytologist* 222: 97–114.
1144 Olson, D. M., E. Dinerstein, E. D. Wikramanayake, N. D. Burgess, G. V. N. Powell, E. C.
1145 Underwood, J. A. D'amico, et al. 2001. Terrestrial Ecoregions of the World: A New

1146 Map of Life on Earth a New Global Map of Terrestrial Ecoregions Provides an
1147 Innovative Tool for Conserving Biodiversity. *BioScience* 51: 933–38.
1148 Pagel, M. 1994. Detecting Correlated Evolution on Phylogenies: A General Method for the
1149 Comparative Analysis of Discrete Characters. *Proceedings of the Royal Society of*
1150 *London. Series B: Biological Sciences* 255: 37–45.
1151 Pound, M. J., A. M. Haywood, U. Salzmann, and J. B. Riding. 2012. Global Vegetation
1152 Dynamics and Latitudinal Temperature Gradients During the Mid to Late Miocene
1153 (15.97 – 5.33 Ma). *Earth Science Reviews* 112: 1–22.
1154 Pound, M. J., A. M. Haywood, U. Salzmann, J. B. Riding, D. J. Lunt, and S. J. Hunter. 2011. A
1155 Tortonian (Late Miocene, 11.61 - 7.25 Ma) Global Vegetation Reconstruction.
1156 *Palaeogeography, Palaeoclimatology, Palaeoecology* 300: 29–45.
1157 Pound, M. J., and U. Salzmann. 2017. Heterogeneity in Global Vegetation and Terrestrial
1158 Climate Change During the Late Eocene to Early Oligocene Transition. *Scientific*
1159 *Reports* 7: 43386.
1160 Prentice, I. C., W. Cramer, S. P. Harrison, R. Leemans, R. A. Monserud, and A. M. Solomon.
1161 1992. A Global Biome Model Based on Plant Physiology and Dominance, Soil
1162 Properties and Climate. *Journal of Biogeography*, 117–34.
1163 Quintero, I. and M. J. Landis. 2019. Interdependent Phenotypic and Biogeographic Evolution
1164 Driven by Biotic Interactions. *Systematic Biology* (accepted).
1165 Ree, R. H., B. R. Moore, C. O. Webb, and M. J. Donoghue. 2005. A Likelihood Framework for
1166 Inferring the Evolution of Geographic Range on Phylogenetic Trees. *Evolution* 59:
1167 2299–2311.

1168 Ree, R. H., and I. Sanmartín. 2009. Prospects and Challenges for Parametric Models in
1169 Historical Biogeographical Inference. *Journal of Biogeography* 36: 1211–20.
1170 Ree, R. H., and S. A. Smith. 2008. Maximum Likelihood Inference of Geographic Range
1171 Evolution by Dispersal, Local Extinction, and Cladogenesis. *Systematic Biology* 57: 4–
1172 14.
1173 Rodrigue, N., H. Philippe, and N. Lartillot. 2008. Uniformization for sampling realizations of
1174 Markov processes: applications to Bayesian implementations of codon substitution
1175 models. *Bioinformatics.* 24: 56-62.
1176 Ronquist, F., S. Klopfstein, L. Vilhelmsen, S. Schulmeister, D. L. Murray, and A. P. Rasnitsyn.
1177 2012. A total-evidence approach to dating with fossils, applied to the early radiation
1178 of the Hymenoptera. *Systematic Biology* 61: 973–99.
1179 Salzmann, U., A. M. Haywood, and D. J. Lunt. 2009. The past is a guide to the future?
1180 Comparing Middle Pliocene vegetation with predicted biome distributions for the
1181 twenty-first century. *Philosophical Transactions: Series A: Mathematical, Physical,*
1182 *and Engineering Sciences* 367: 189–204.
1183 Salzmann, U., A. M. Haywood, D. J. Lunt, P. J. Valdes, and D. J. Hill. 2008. A new global biome
1184 reconstruction and data-model comparison for the Middle Pliocene. *Global Ecology*
1185 *and Biogeography* 17: 432–47.
1186 Schmerler, S. B., W. L. Clement, J. M. Beaulieu, D. S. Chatelet, L. Sack, M. J. Donoghue, and E. J.
1187 Edwards. 2012. Evolution of Leaf Form Correlates with Tropical–Temperate
1188 Transitions in *Viburnum* (Adoxaceae). *Proceedings of the Royal Society B: Biological*
1189 *Sciences* 279: 3905–13.

1190 Scoffoni, C., D. S. Chatelet, J. Pasquet-Kok, M. Rawls, M. J. Donoghue, E. J. Edwards, and L.
1191 Sack. 2016. Hydraulic Basis for the Evolution of Photosynthetic Productivity. *Nature*
1192 *Plants* 2: 16072.
1193 Spriggs, E. L., W. L. Clement, P. W. Sweeney, S. Madriñán, E. J. Edwards, and M. J. Donoghue.
1194 2015. Temperate Radiations and Dying Embers of a Tropical Past: The
1195 Diversification of Viburnum. *New Phytologist* 207: 340–54.
1196 Sukumaran, J., E. P. Economo, and L. L. Knowles. 2015. Machine Learning Biogeographic
1197 Processes from Biotic Patterns: A New Trait-Dependent Dispersal and
1198 Diversification Model with Model Choice by Simulation-Trained Discriminant
1199 Analysis. *Systematic Biology* 65: 525–545.
1200 Sukumaran, J., and L. L. Knowles. 2018. Trait-Dependent Biogeography:(Re) Integrating
1201 Biology into Probabilistic Historical Biogeographical Models. *Trends in Ecology &*
1202 *Evolution* 33: 390–98.
1203 Tagliacollo, V. A., S. M. Duke-Sylvester, W. A. Matamoros, P. Chakrabarty, and J. S. Albert.
1204 2015. Coordinated Dispersal and Pre-Isthmian Assembly of the Central American
1205 Ichthyofauna. *Systematic Biology* 66: 183–96.
1206 Tiffney, B. H. 1985a. Perspectives on the origin of the floristic similarity between eastern
1207 Asia and eastern North America. *J. Arnold Arbor.* 66: 73–94.
1208 Tiffney, B. H. 1985b. The Eocene North Atlantic Land Bridge: Its importance in Tertiary and
1209 modern phytogeography of the Northern Hemisphere. *J. Arnold Arbor.* 66: 243–273.
1210 Tiffney, B. H. and S. R. Manchester. 2001. The use of geological and paleontological evidence
1211 in evaluating plant phylogeographic hypotheses in the Northern Hemisphere
1212 Tertiary. *Int. J. Plant. Sci.* 162: S3–S17.

1213 Verdinelli, I., and L. Wasserman. 1995. Computing Bayes Factors Using a Generalization of
1214 the Savage-Dickey Density Ratio. *Journal of the American Statistical Association* 90:
1215 614–18.
1216 Webb, C. O., and R. H. Ree. 2012. Historical Biogeography Inference in Malesia. In *Biotic*
1217 *Evolution and Environmental Change in Southeast Asia*, edited by D. Gower, K.
1218 Johnson, J. Richardson, B. Rosen, L. Ruber, and S. Williams, 191–215. Cambridge
1219 University Press.
1220 Weeks, A., F. Zapata, S. K. Pell, D. C. Daly, J. D. Mitchell, and P. V. A. Fine. 2014. To Move or to
1221 Evolve: Contrasting Patterns of Intercontinental Connectivity and Climatic Niche
1222 Evolution in 'Terebinthaceae' (Anacardiaceae and Burseraceae). *Frontiers in*
1223 *Genetics* 5: 409.
1224 Whittaker, R. H. 1970. *Communities and Ecosystems*. Macmillan Company.
1225 Wickham, H. 2016. *ggplot2: Elegant Graphics for Data Analysis*. Springer.
1226 Wiens, J. J., and M. J. Donoghue. 2004. Historical Biogeography, Ecology and Species
1227 Richness. *Trends in Ecology & Evolution* 19: 639–44.
1228 Willis, K., and J. McElwain. 2014. *The Evolution of Plants*. Oxford University Press.
1229 Wolfe, J. A. 1975. Some aspects of the plant geography of the Northern Hemisphere during
1230 the Late Cretaceous and Tertiary. *Ann. Missouri Bot. Gard.* 62: 264–279.
1231 Wolfe, J. A. 1985. Distribution of Major Vegetational Types During the Tertiary. *The Carbon*
1232 *Cycle and Atmospheric CO2: Natural Variations Archean to Present* 32: 357–75.
1233 Xie, W., P. O. Lewis, Y. Fan, L. Kuo, and M.-H. Chen. 2011. Improving marginal likelihood
1234 estimation for Bayesian phylogenetic model selection. *Syst. Biol.* 60: 150-160.

TABLE CAPTIONS

Table 1. Regional biome shift parameter estimates. Posterior median estimates are in bold and 95% highest posterior densities are in brackets. Fixed parameters under the *Null Biome* analysis do not have brackets.

FIGURE CAPTIONS

Figure 1. Cartoon of the relationship between paleobiome structure and a regional biome shift process. The left and right panels are aligned to the same geological time scale that is divided into a Hot (red) interval followed by a Cold (blue) interval. (A) Maps of paleobiome structure with two regions, East (E) and West (W), and two focal biomes of interest, Hot (H) and Cold (C), in which the expansive Hot biome is replaced by the Cold biome as the East and West regions separate. (B) Paleobiome adjacency matrices encode the availability of biomes within regions and the connectivity of biomes between regions based on whether paleobiome features are strong (dark) or weak (light). Diagonal elements reflect biome availability within regions while off-diagonal elements report biome connectivity between regions. (C) Two possible regional biome shift histories for a phylogeny with a western, hot-adapted (HW) origin. Lineages shift between biomes at rates that depend on the availability of biomes within the lineage's current region and disperse between regions at rates that depend on connectivity of the lineage's current biome between regions. The two histories require (top) or do not require (bottom) evolutionary events to be congruent

with paleobiome structure. (D) Time-dependent biome shift rates for the four possible events: HW to CW, CW to HW, HE to CE, and CE to HE. (E) Time-dependent dispersal rates for the four possible events: HW to HE, HE to HW, CW to CE, and CE to CW.

Figure 2. Availability and connectivity of biomes from Late Cretaceous (100 Ma) to Recent. Adjacency matrices are used to structure the time-stratified phylogenetic biome shift process. Rows correspond to eight major time intervals, while columns correspond to regional features, specifically uninformative features (black), simple geographical features (brown), or features involving the tropical (red), warm temperate (green), and cold temperate (blue) forest biomes. The matrix for each time and feature encodes the availability of (the diagonal) and the connectivity between (off-diagonal) regions for that feature at that time, where matrix rows and columns correspond to source and destination regions, respectively. Cells representing availability and connectivity are shaded to represent those features as being strong (dark), weak (medium), or marginal (light).

Figure 3. Stationary distribution of biome-region states under the paleobiome model. The stationary probabilities across biome-regions (y-axis) vary with respect to time (x-axis). Stationary probabilities were computed assuming that biome and region shifts are expected to occur in equal proportion ($\beta = \delta = 0.5$), that lineages tend to shift and disperse in a manner than depends heavily on the paleobiome structure ($w_U = 0.04$, $w_G = 0.16$, and $w_B = 0.8$), and that biomes with strong presences primarily define the structure of biome graphs ($y = 0.1$). Parameters were chosen to show interesting variation. Note, all stationary probabilities would be equal over all times if $w_U = 1$.

Figure 4. Simulation experiment results. One hundred datasets were simulated under five conditions that varied the strength of w_B, then fitted to the paleobiome model to assess model performance. (A) Markers show the true simulated strength for w_B (closed square), the posterior median values estimated from simulated replicates (open circles), the median of those posterior medians (closed circle), and the upper and lower bounds of the 95% highest posterior density (open triangles). The coverage frequency reports the proportion of simulation analyses in which the simulating value of w_B is falls within the 95% highest posterior density. (B) Bars report the proportions of simulated datasets that supported the model where $w_B > 0$, categorized by the strength of that support in terms of Bayes factors (Jeffreys 1961).

Figure 5. Ancestral biome-region state estimates for *Viburnum*. Estimates produced under (A) *Paleobiome*, (B) *Modern Biome*, and (C) *Null Biome* settings. Colored pie charts report posterior support for the three most probable biome-region states per node. Pie charts for root state probabilities are magnified to improve visibility. Vertical white and gray bands correspond to major geological timeframes referenced in this study.

Figure 6. Ancestral proportions of lineage state frequencies through time for *Viburnum*. The left column (A–C) shows the lineages biome-region states, where regions differ by color and biomes differ by shading (see legend). Proportions of reconstructed lineages in each biome-region state are shown for estimates under the *Paleobiome* (A), *Modern Biome* (B), and *Null Biome* (C) settings. The right column (D–F) shows the proportion of lineages with

biome states that match (dark) or mismatch (light) the non-marginal biomes that are locally accessible given any lineage's location, as defined under the Paleobiome structure (see main text for details). Proportions of reconstructed lineages with biome match and mismatch scores are shown for estimates under the *Paleobiome* (D), *Modern Biome* (E), and *Null Biome* (F) settings.

Figure 7. Stationary probabilities for the *Viburnum* root state during the Late Cretaceous. Posterior stationary probabilities for $\pi(m_{\text{root}})$ are given for each biome structure model (grouped rows) and for each biome-region state (colors) as posterior means (points) and credible intervals (HPD80, thick lines; HPD95, thin lines).

Figure 8. Proportions of inferred events and event series across major time intervals for *Viburnum*. Posterior proportions are presented as posterior means (points) and credible intervals (HPD80, thick lines; HPD95, thin lines). The left column (A–C) presents the proportions of estimated biome shift and dispersal events with respect to time, showing only the eight biome shift and dispersal events among the warm and cold temperate forests of East Asia and North America. Proportions of events are shown for inferences under the *Paleobiome* (A), *Modern Biome* (B), and *Null Biome* (C) settings. The right column (D–F) shows the proportions of the six types of event series with respect to time (defined in main text). Each event series type is labeled with a 'state triplet' to indicate either transitions in the biome (A, B, C) or region (X, Y, Z) state.

1326 Table 1

	Biome structure		
Parameter	*Paleo*	*Modern*	*Null*
μ	**0.06** [0.03,0.10]	**0.05** [0.03,0.09]	**0.03** [0.02,0.06]
f_β	**0.85** [0.75,0.94]	**0.83** [0.69,0.93]	**0.92** [0.85,0.97]
f_δ	**0.15** [0.06,0.25]	**0.17** [0.07,0.31]	**0.08** [0.03,0.15]
β_{TW}	**0.67** [0.20,1.00]	**0.50** [0.05,0.95]	**0.54** [0.10,1.00]
β_{WC}	**0.81** [0.47,1.00]	**0.81** [0.48,1.00]	**0.74** [0.39,1.00]
β_{CW}	**0.28** [0.09,0.62]	**0.39** [0.11,0.85]	**0.31** [0.08,0.66]
β_{WT}	**0.38** [0.01,0.80]	**0.65** [0.34,1.00]	**0.72** [0.33,1.00]
w_U	**0.01** [0.00,0.07]	**0.02** [0.00,0.08]	**1**
w_G	**0.04** [0.00,0.18]	**0.04** [0.00,0.20]	**0**
w_B	**0.94** [0.78,1.00]	**0.93** [0.76,1.00]	**0**
y	**0.65** [0.27,0.99]	**0.52** [0.09,0.95]	**1**

1327

1328 Figure 1

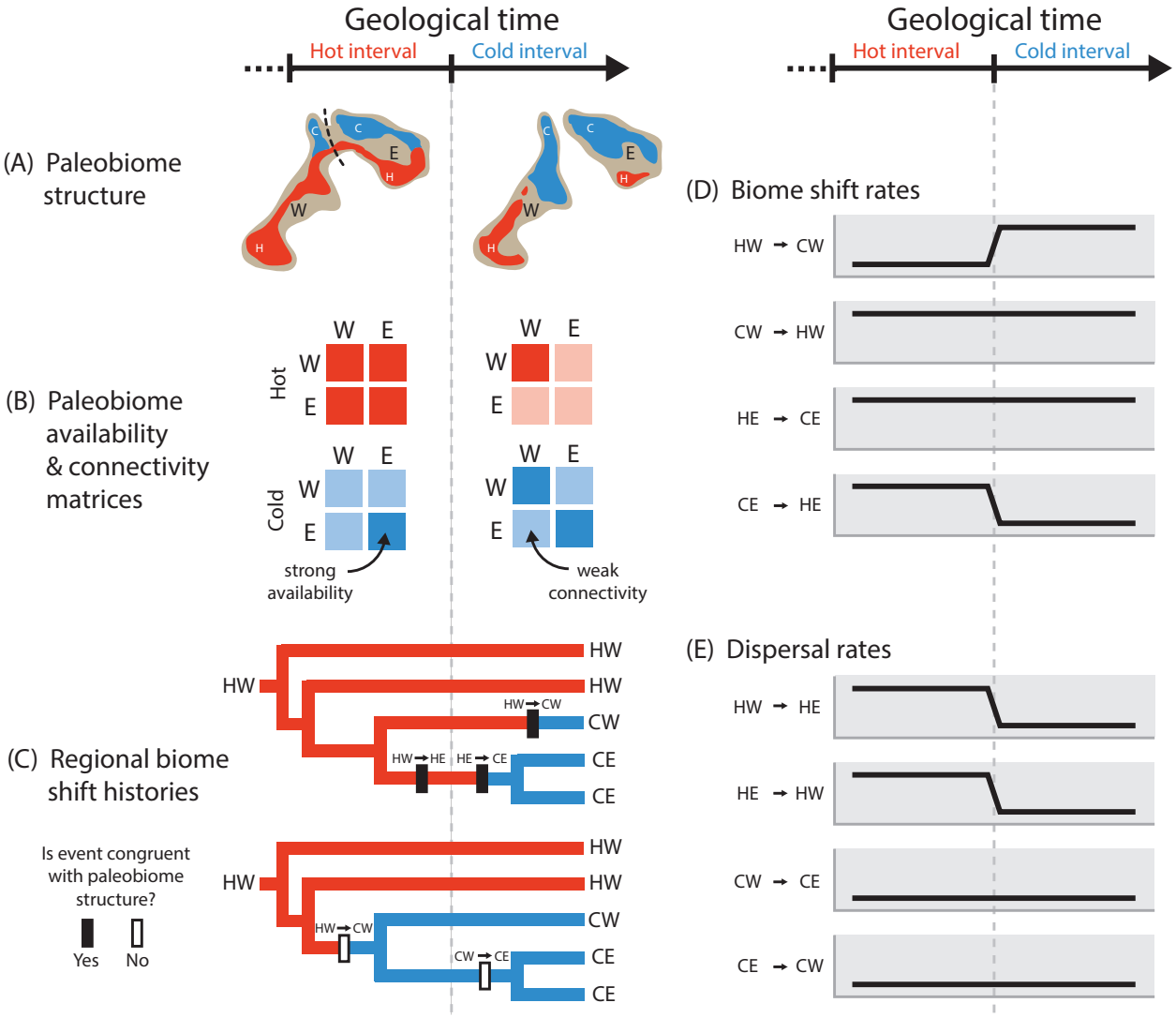

1329

1330 Figure 2

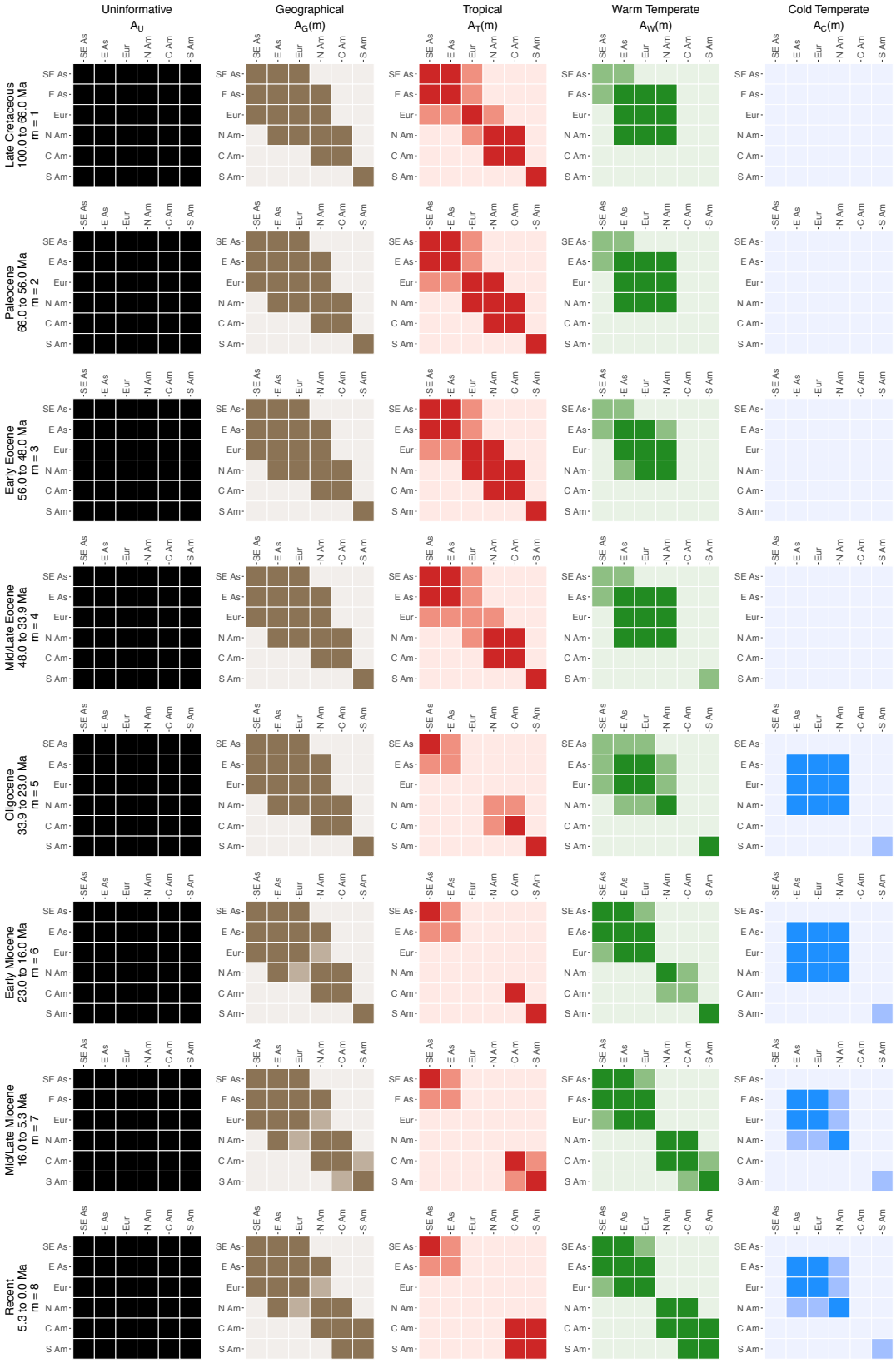

1331

1332 Figure 3

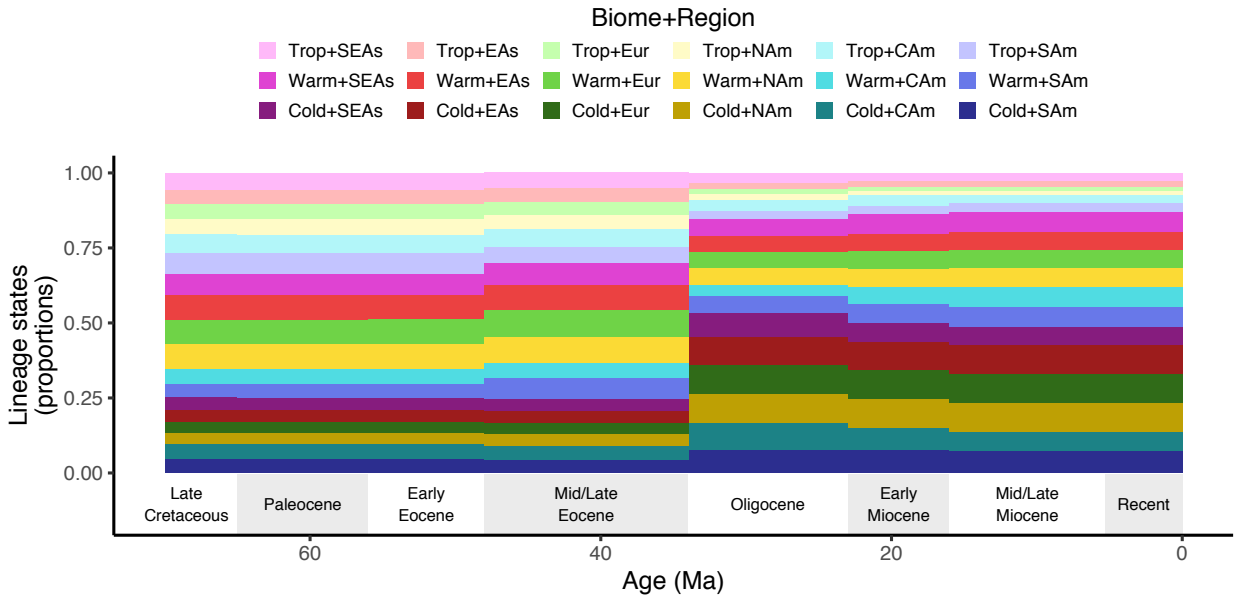

1333

1334 Figure 4

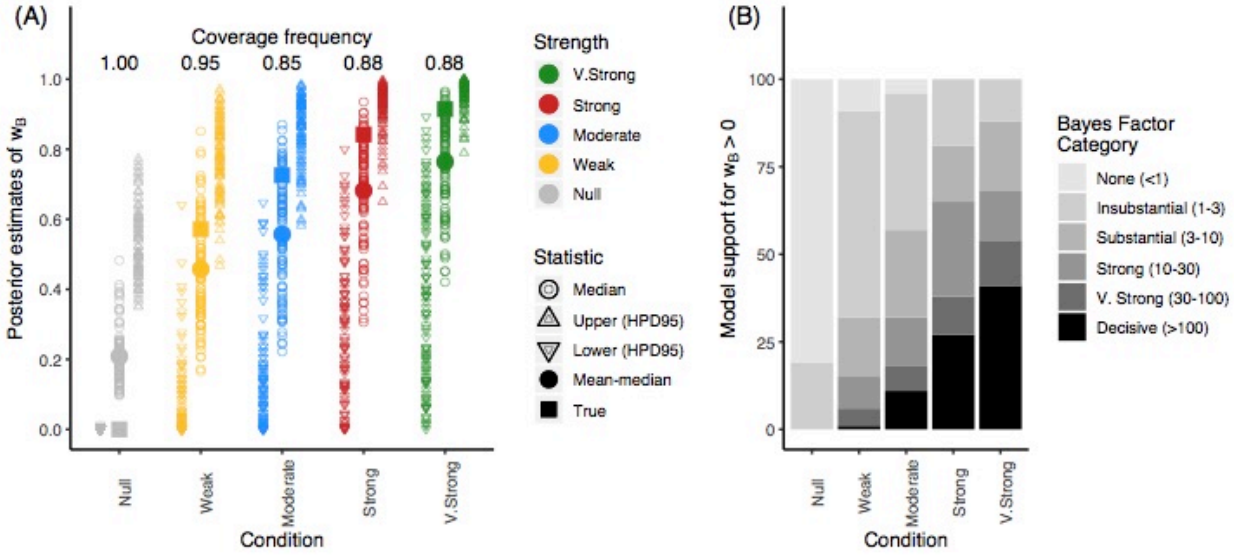

1335

1336 Figure 5

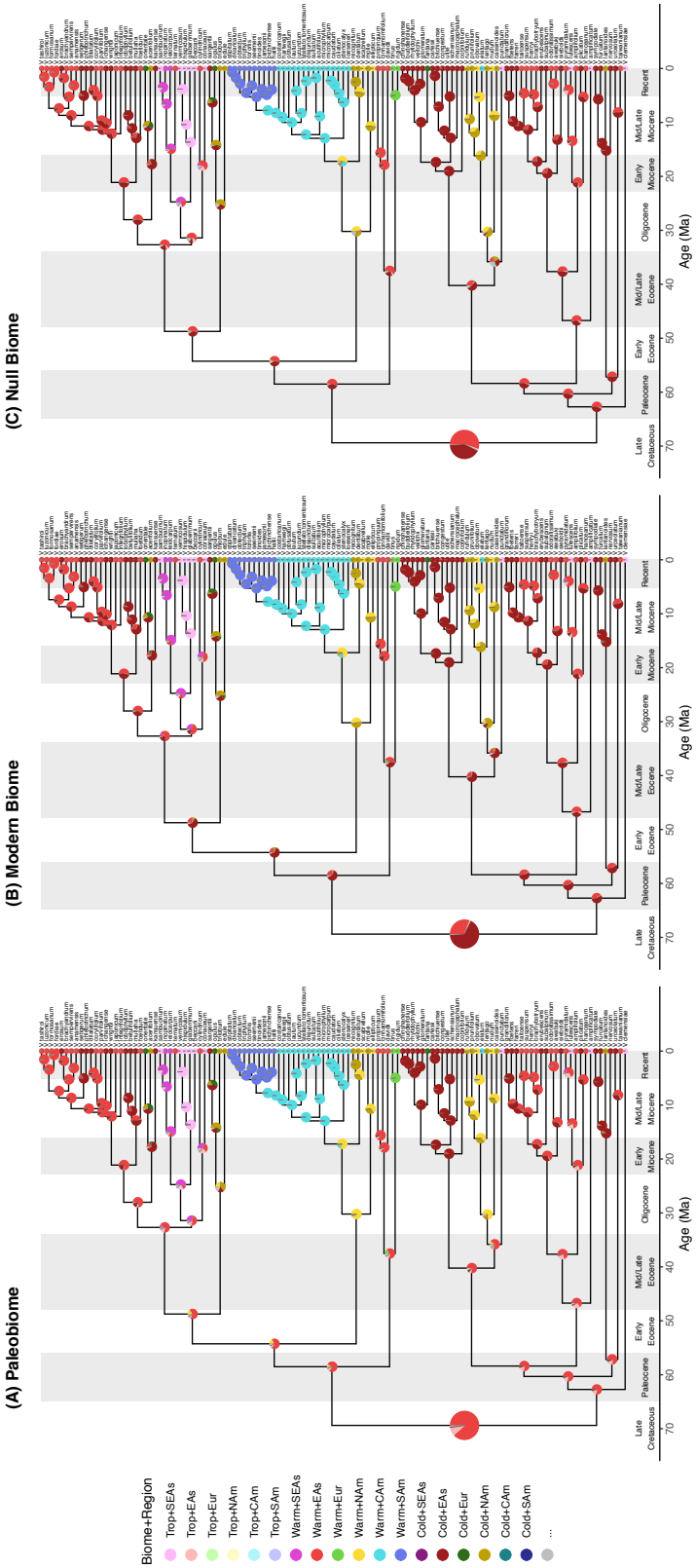

1337

1338 Figure 6

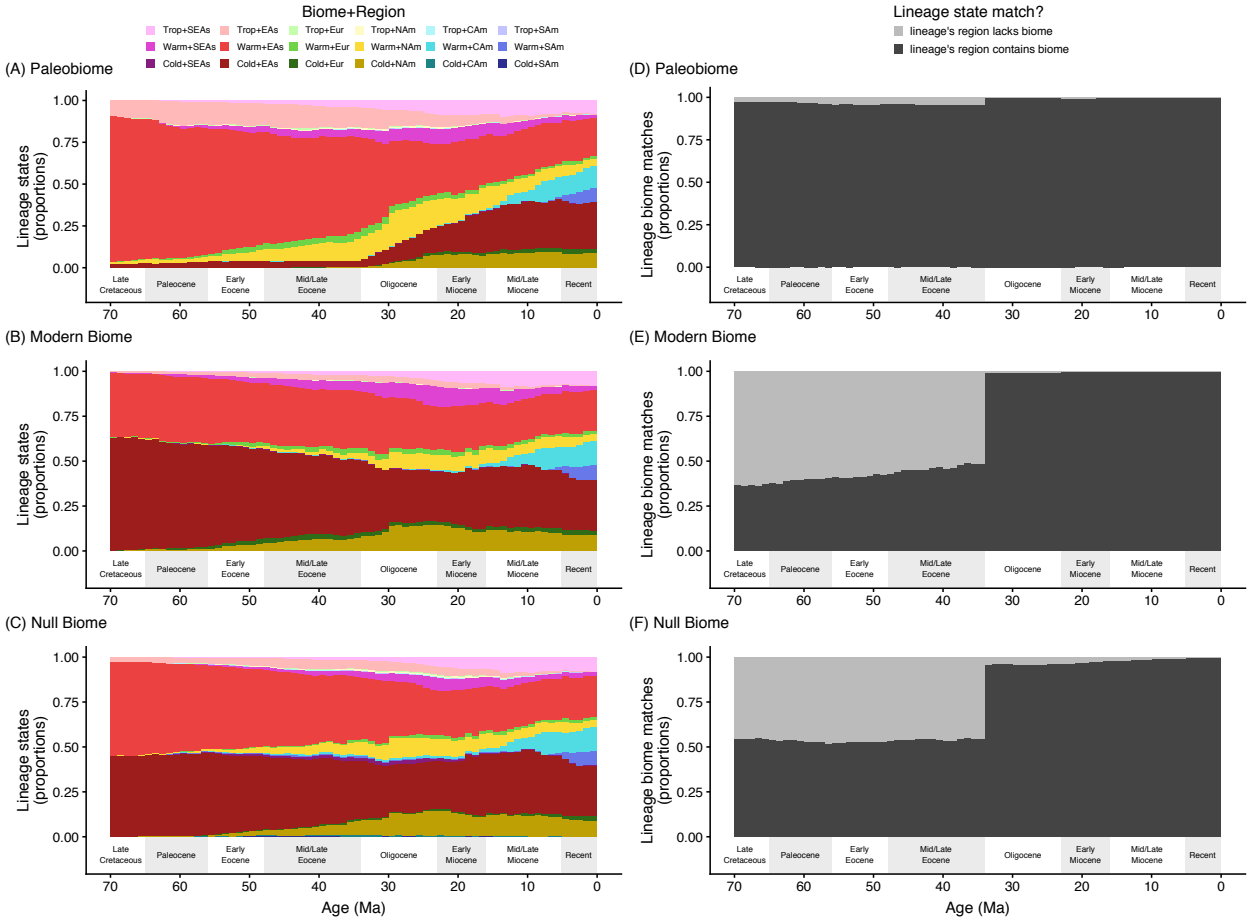

1339

1340 Figure 7

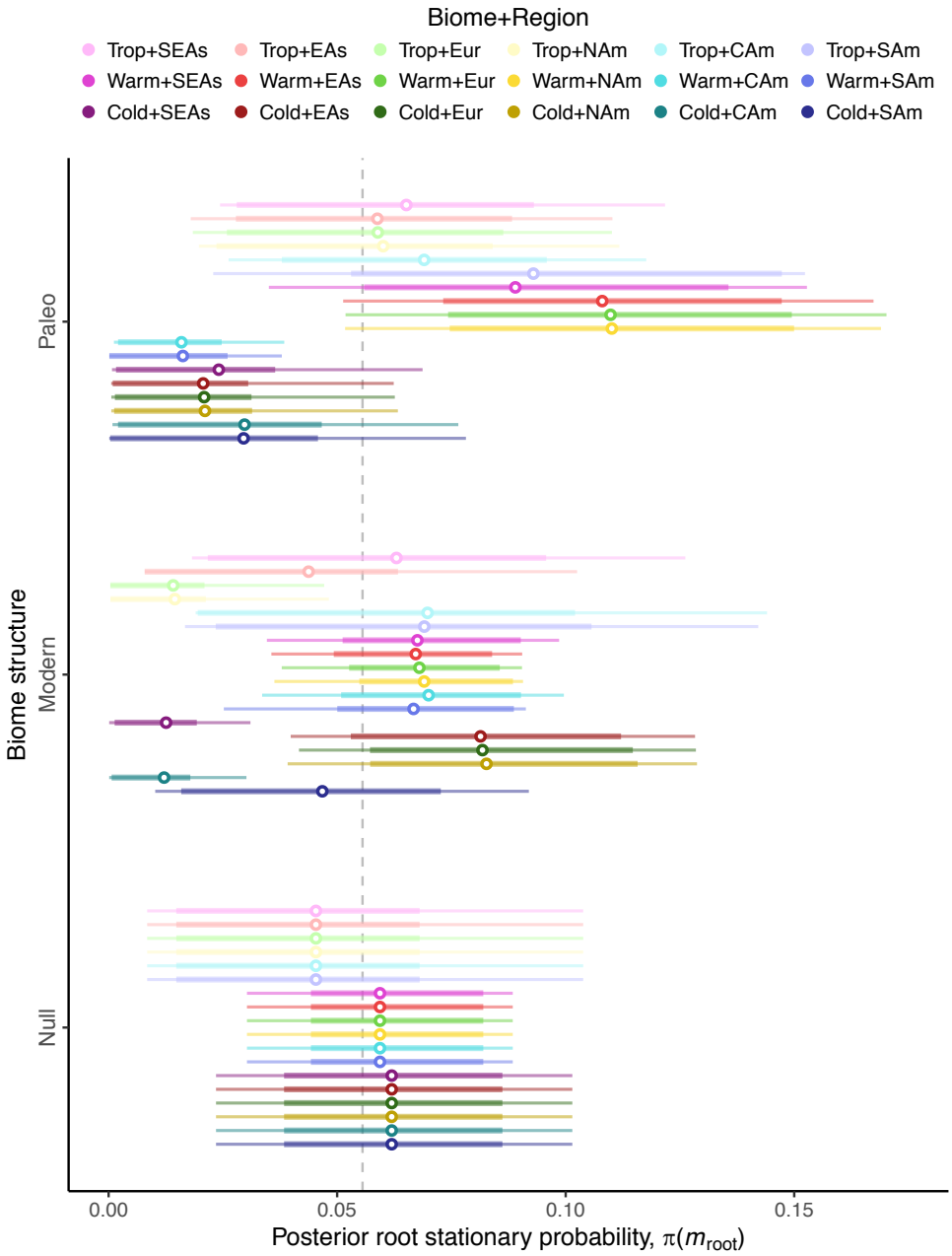

1341

1342 Figure 8

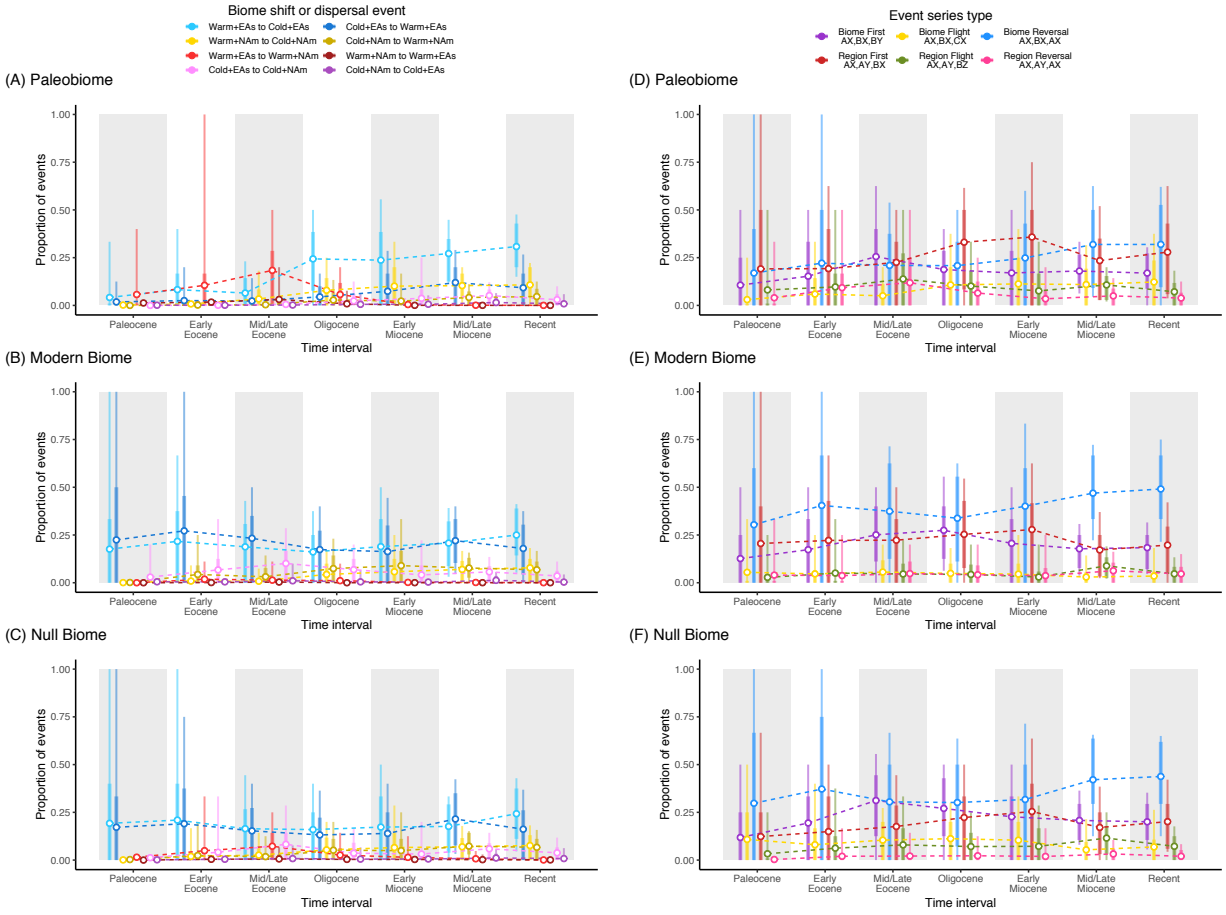

1343